Rhodes College Digital Archives - DLynx

Design and Synthesis of Novel LpxC Inhibitors to Impede Outer Membrane Formation in Gram-Negative Bacteria

Authors	Pajarillo, Andrea Olivia
Download date	2025-08-04 16:08:04
Link to Item	

Design and Synthesis of Novel LpxC Inhibitors to Impede
Outer Membrane Formation in Gram-Negative Bacteria

Andrea Olivia Pajarillo

Department of Chemistry
Rhodes College
Memphis, Tennessee

2018

Submitted in partial fulfillment of the requirements for the
Bachelor of Science degree with Honors in Chemistry

This Honors paper by Andrea Pajarillo has been read

and approved for Honors in Chemistry.

Dr. Larryn W. Peterson
Project Advisor

_____

Dr. Mauricio Cafiero
Second Reader

_____

Dr. Bayly Wheeler
Extra-Departmental Reader

_____

Dr. Mauricio Cafiero
Department Chair

_____

ACKNOWLEDGEMENTS

CONTENTS

LIST OF FIGURES

LIST OF SCHEMES

LIST OF TABLES

ABSTRACT

Design and Synthesis of Novel LpxC Inhibitors to Impede Outer Membrane Formation in

Gram-Negative Bacteria

By

Andrea Olivia Pajarillo

The increasing global incidence of antibiotic-resistant Gram-negative bacteria necessitates the discovery of new treatment mechanisms to combat such untreatable and deadly infections. One promising target is LpxC, a highly conserved Gram-negative enzyme which performs a crucial step in the lipid A biosynthetic pathway. Lipid A serves as the anchor for lipopolysaccharides on the Gram-negative outer membrane and is essential to the structural integrity and viability of the bacterium. The LpxC active site is comprised of a zinc ion, a polar region, and a hydrophobic passage. A library of analogs with varying hydrophobic tails similar in structure to the natural substrate were designed and synthesized with the goal of optimizing binding within the active site. Two new analogs (**DP-001** and **DP-002**) were added to the existing LpxC inhibitor library which contain a phenyl propargyl ether tail as a hydrophobic moiety. The phenyl propargyl ether tail was synthesized and a new approach was developed to achieve hydroxamic acid conversion. Both **DP-001** and **DP-002** will be tested alongside the rest of the Peterson library against various strains of Gram-negative and Gram-positive bacteria for antimicrobial activity.

I give permission for public access to my Honors paper and for any copying or digitization to be done at the discretion of the College Archivist and/or the College Librarian.

Signed_____

Andrea Olivia Pajarillo

Date _____

Introduction

Incidences of multidrug-resistant pathogens have increased on a global basis, creating one of the greatest crises in the modern medical field.[1] Various strains of bacteria have exhibited resistance to even last-resort antibiotics, causing life-threatening infections which do not respond to existing treatments.[2] In the US alone, at least 2 million cases of multidrug resistant bacterial infections occur each year, resulting in approximately 23,000 deaths per annum.[3] The antibiotic resistance crisis can be attributed to overuse and misuse of antibiotics as well as a decrease in antibiotic drug research by pharmaceutical companies over time. The high economic risk of antibiotic research and discovery paired with the eventual expiration of the drugs have driven pharmaceutical companies to more profitable ventures, leaving less novel antibiotics available to combat dangerous bacterial infections.[1]

Approximately 14% of hospital acquired infections (HAIs) in acute care facilities are caused by antibiotic-resistant pathogens.[4] Though not the initial cause of hospitalization, HAIs caused by multidrug-resistant bacteria lead to longer hospital, greater medical costs, and higher mortality rates when compared to HAIs caused by antibiotic-sensitive pathogens.[5] Often, infections can cause sepsis, an overactivation of the immune system in response to a pathogen, that causes organ failure and death.[6]

Gram-negative bacteria that exhibit multidrug resistance are particularly dangerous, as the signature outer membrane blocks entry of various antibiotics and limits an already small list of treatment options.[7] Particularly dangerous strains of Gram-negative bacteria include *A. baumannii*, *K. pneumoniae.*, *E. coli*, and *P. aeruginosa*,

which all exhibit worryingly high levels of resistance to most or all available antibiotic treatments.[3]

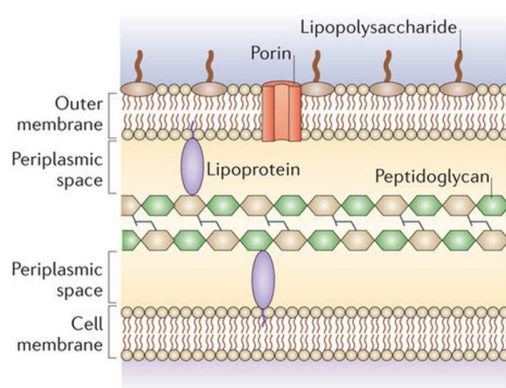The Gram-negative outer membrane is studded with lipopolysaccharides (LPS) that are the main structural component of the membrane (Figure 1).[8] Each LPS molecule consists of three sections: an O-antigen, a core oligosaccharide, and a toxic lipid A anchor embedded in the membrane.[9] Lipid A is a powerful endotoxin that contributes to bacterial resistance to antibiotics and detergents.[10] As an endotoxin, lipid A is the only LPS component recognized by the innate immune system, and can overactivate the immune inflammatory response and lead to sepsis.[11] Various studies have shown that mutant bacteria lacking lipid A are inviable, while other mutant strains with inhibited lipid A biosynthesis were more susceptible to antibiotic treatment.[12] Some suggested mechanisms for the increase in antibiotic sensitivity and cell death include improper buildup of LPS components.[9] As such, prevention of lipid A biosynthesis is a promising method for antimicrobial treatment.

Figure 1: Gram negative membrane with LPS.[8]

One approach to inhibition of lipid A formation is targeting the enzyme UDP-(3-O-((R)-3-hydroxymyristoyl))-N-acetylglucosamine deacetylase, or LpxC, which is responsible for the first committed step of lipid A synthesis
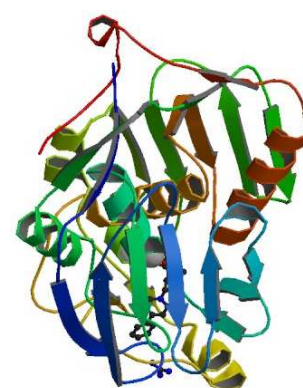

Figure 2: LpxC crystal structure with bound inhibitor.[18]

(Figure 2). Inhibition of LpxC prevents LPS formation, rendering the bacterium more

sensitive to antibiotic treatment and, in many cases, making it inviable.[9] LpxC is also

highly conserved within Gram-negative strains and shares no homology with mammalian

enzymes, making it an attractive target for antimicrobial treatment.[13]

     Our research group has analyzed the crystal structure of the LpxC active site and

found three target areas: a Zn^{2+} ion, a polar region, and a hydrophobic passage.[14] The

strongest interaction occurs with the Zn^{2+} ion.[13] The strongest previously synthesized

LpxC inhibitors found in literature all share a hydroxamate head group that binds

strongly to the Zn^{2+} ion.[15] In fact, the hydroxamate ion has a distinct thermodynamic

advantage over an acetate ion as a Zn^{2+} binding motif, with the hydroxamate forming a

five-membered ring completed by the Zn^{2+} ion.[16] An aromatic tail is attached to the

hydroxamate in order to fill the hydrophobic passage and improve binding specificity

(Figure 3).[17] Of these inhibitors, LPC-058 has shown the best IC_{50} values against
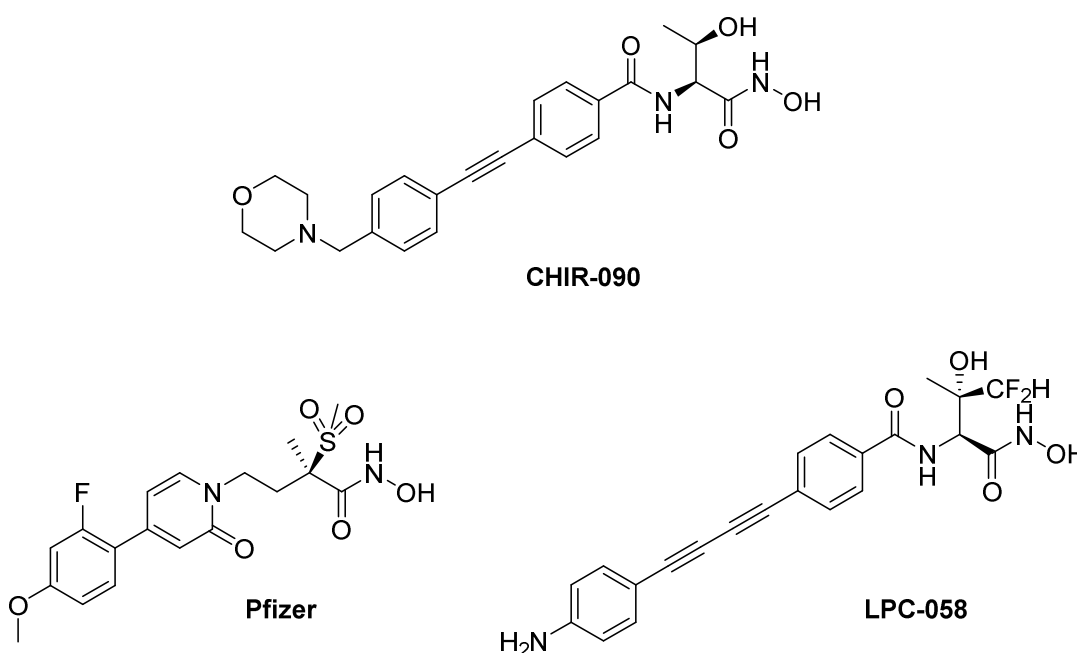

Figure 3: Previously developed LpxC inhibitors.

Acinetobacter baumannii at 0.39 µg/mL, exhibiting better inhibitory activity than CHIR-090 across all tested Gram-negative bacteria by factors of 5- to 55-fold.[18] However, most published LpxC inhibitors only target the Zn^{2+} ion and hydrophobic passage, and do not contain structures capable of interacting within the nucleoside-binding polar region.[19] CHIR-090 has an IC_{50} value of less than 2.1 nM, while the Pfizer inhibitor exhibits 1.1 nM IC_{50} in wild type *P. aeruginosa*.[20] The strongest inhibitors contain a large group that sterically occupies the polar site such as the difluorosubstituted methyl of LPC-058, implying that the interaction within this pocket is crucial to LpxC inhibition.[21]

Rationale

Potential inhibitors of LpxC were designed by various members of the Peterson lab group capable of targeting two or more regions in the active site. The general structure of our design library was based on the LpxC natural substrate, which consists of a nucleoside, a diphosphate linker, a glucosamine, and a long hydrocarbon tail (Figure 4A). All proposed analogs share a hydroxamate head group as a Zn^{2+} binding motif, but differ in inclusion of a nucleoside and in type of hydrophobic tail (Figure 4B). Early proposed structures considered both ether and triazole linkages to connect the nucleoside
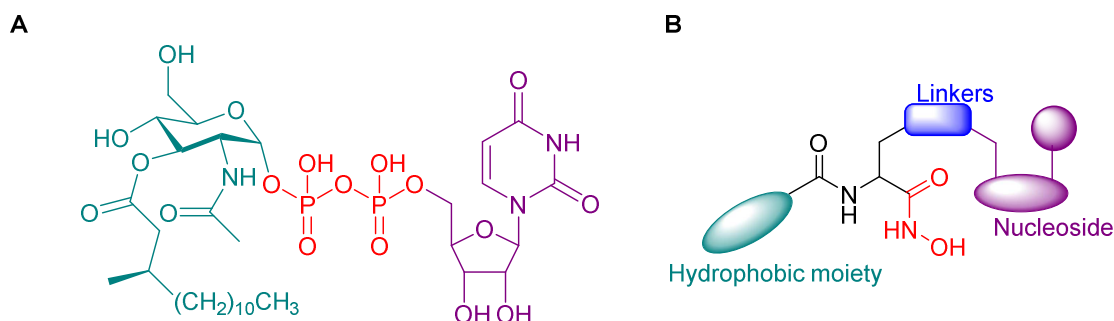
Figure 4: **A**) The structure of the LpxC natural substrate was used to create **B**) the general structure of analog library.

to the hydroxamate and hydrophobic tail. However, computational studies performed by the Cafiero lab (Table 1) have found that the triazole linkage contributes to the hydroxamate-Zn^{2+} interaction (Figure 5).[14]

    Due to the relative ease of synthesis of the triazole group compared to ether formation, ether-linked structures were abandoned in favor of the triazole-containing analogs. The current Peterson library consists of nucleoside and non-nucleoside compounds with hydroxamic acids and differing hydrophobic tails (Figure 6).

Table 1: Interaction energies of **SA-001** and **SA-002** in kcal/mol

Molecule	Total IE (kcal/mol)
SA-001	-283
SA-002	-606

SA-001   **SA-002**
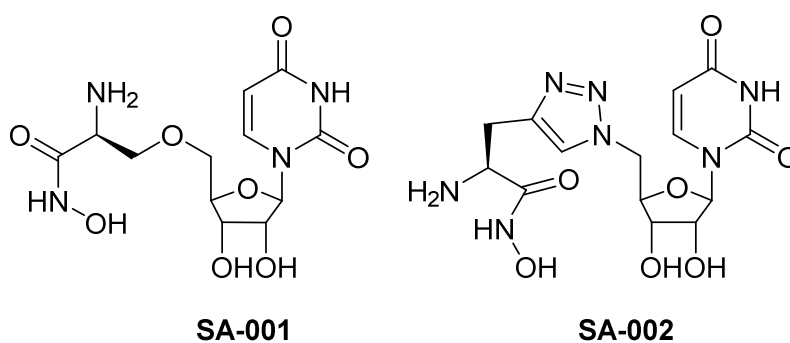
Figure 5: The triazole-linked compound (**SA-002**) showed a more negative interaction energy than the ether-linked compound (**SA-001**) in computational analysis, indicating better binding in the active site (**Table 1**).[14]
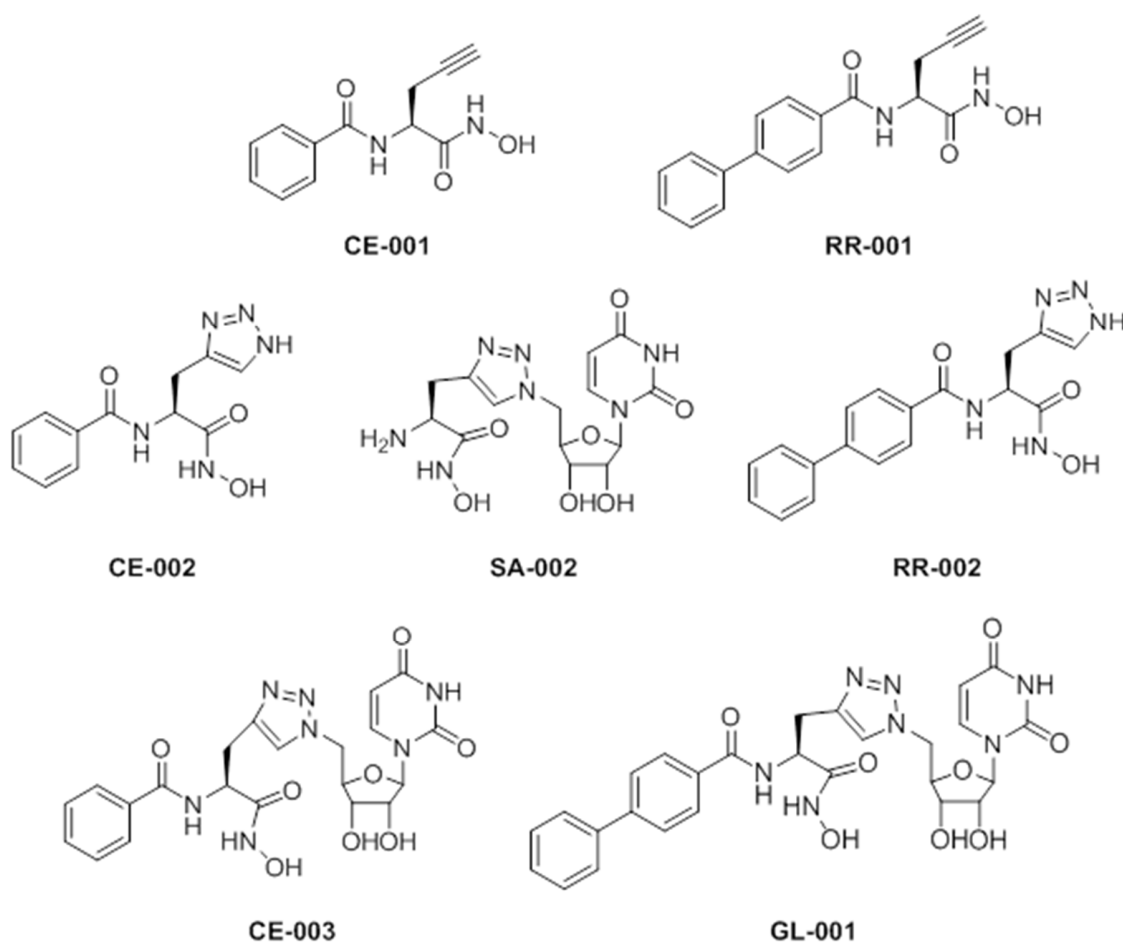
Figure 6: Potential LpxC inhibitor library developed by the Peterson lab.

While **SA-002** showed great promise in LpxC binding during computational trials, **GL-001** was developed to fill the hydrophobic passage of the active site and increase specificity.[15] Non-nucleoside molecules have also been synthesized by my colleagues Rebeca Roldan and Carter Embry which contain an alkyne (**RR-001** and **CE-001**). In the future, triazole analogs of these non-nucleoside compounds will also be synthesized. These compounds will be tested alongside the nucleoside-based analogs in order to determine the degree to which the nucleoside and triazole group contribute to LpxC inhibition.

Incorporation of a hydrophobic tail to bind in the active site offers both design and synthetic challenges. The amino acid sequence in these tunnels differs across many Gram-negative strains, thus varying passage shape.[22] In order to achieve broad spectrum activity against different Gram-negative species, the tail must be able to fit within a variety of hydrophobic passages and resolve any differences. Many research groups have found that more linear tails can account for slight variations in the hydrophobic tunnel, resulting in a wide variety of tails with aromatic groups bound by acetylene or diacetylene.[23] However, many inhibitors which include diacetylene groups, including the previously mentioned CHIR-090, showed low aqueous solubility as well as *in vitro* cytotoxicity. In place of the diacetylene and acetylene tails, a flexible propargyl ether group was designed which could specifically inhibit *P. aeruginosa* LpxC.[24] The Piizi compound A, which includes the propargyl ether tail, showed a strong IC_{50} value of 0.006 μM, as well as good aqueous solubility with no cytotoxic effects (Figure 7).
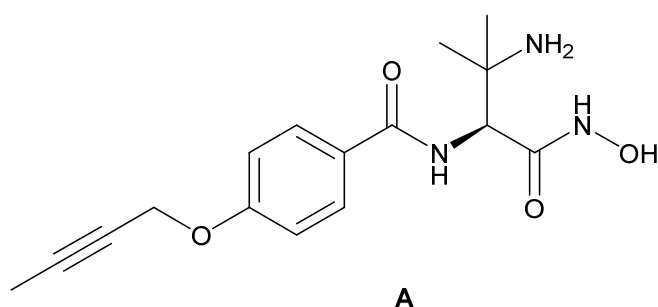

Figure 7: Compound **A** from Piizi, et al. contains a phenyl propargyl ether tail as a hydrophobic moiety. Wild type *P. aeruginosa* IC_{50} was 1.5 nM and in MDR *P. aeruginosa* MIC_{90} was 2 μg/mL.[22]

Purpose

This honors research works to improve and expand upon the current Peterson library by optimizing necessary reactions such as the azidonucleoside synthesis and developing new potential inhibitors. With the success of the Piizi tail in mind, **DP-001** and its corresponding alkyne **DP-002** were designed and synthesized as potential LpxC inhibitors (Figure 8). While **DP-002** was fully synthesized and saved for future testing and characterization, **DP-001** was synthesized to the protected stage just before the final compound. Unlike the commercially available benzoic acids used in **GL-001** and **CE-003**, the DP tail had to be synthesized completely prior to coupling with the propargylglycine. Additionally, a new synthetic procedure was implemented regarding the hydroxamate conversion and will be detailed in this paper.
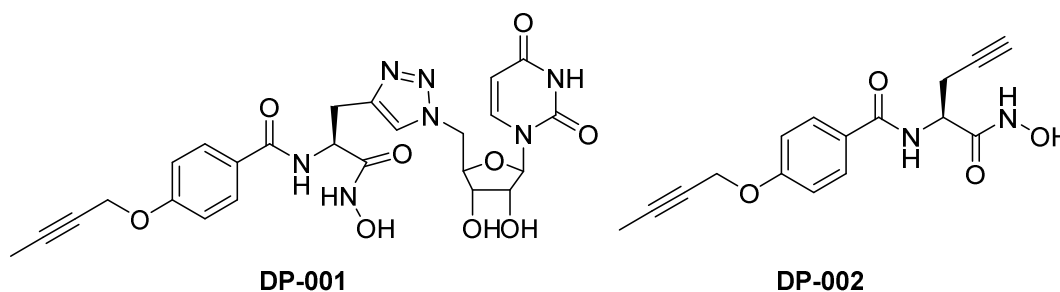

Figure 8: **DP-001** and **DP-002** contain a phenyl propargyl ether tail which has shown good antimicrobial activity in *P. aeruginosa*.[23]

Experimentals

All anhydrous solvents used were obtained from commercial sources and stored in Sure-seal bottles. Necessary reagents and other solvents were acquired from Sigma-Aldrich and Acros. Fmoc-L-Propargylglycine was purchased from AK Scientific. Unless otherwise stated, all reactions were done under ultra-pure argon in standard glass round bottom flasks. Column chromatography was executed using silica gel (Silicycle 55-65 Å). Proton (^{1}H) and carbon (^{13}C) NMR spectra were taken using a Varian 400 MHz spectrometer. Chemical shifts (δ) were reported in parts per million (ppm) and referenced to ^{1}H (CDCl$_3$ at 7.26, DMSO at 2.50, CD$_3$OD at 3.31) and ^{13}C (CDCl$_3$ at 77.16, DMSO at 39.52, and CD$_3$OD at 49.00).

A. Ketal protection of uridine

1-((3aR,4R,6R,6aR)-6-(hydroxymethyl)-2,2-dimethyltetrahydrofuro[3,4-d][1,3]dioxol-4-yl)pyrimidine-2,4(1H,3H)-dione (1)

Commercially available uridine (2.63 g, 10.8 mmol, 1 EQ) was dissolved in acetone (150 mL) at rt. Concentrated H$_2$SO$_4$ (1.31 mL, 24.6 mmol, 2.3 EQ) was added dropwise. The reaction was stirred at rt for 1.5 hours, neutralized with TEA (3.75 mL), and concentrated under reduced pressure. The crude product was purified by silica gel column chromatography (MeOH:CH$_2$Cl$_2$, 0-8%) to afford alcohol **1** (2.95 g, 96 % yield) as a white solid. R$_f$ (10% MeOH:CH$_2$Cl$_2$) = 0.42

^{1}HNMR (400 MHz, DMSO): δ 1.27 (s, 3 H), 1.47 (s, 3 H), 3.30 (s, 2 H), 4.05 (s, 1 H), 4.72 (s, 1 H), 4.87 (s, 1 H), 5.05 (s, 1 H), 5.61 (s, 1 H), 5.81 (s, 1 H), 7.77 (s, 1 H), 11.36 (s, 1 H)

^{13}CNMR (100.5 MHz, DMSO): δ 25.63, 27.49, 61.70, 80.91, 84.11, 86.95, 91.55, 102.17, 113.40, 142.35, 150.76, 163.60

The ^{1}HNMR and ^{13}CNMR correspond to the literature data.[25]

B. Tosylation of protected uridine

((3aR,4R,6R,6aR)-6-(2,4-dioxo-3,4-dihydropyrimidin-1(2H)-yl)-2,2-dimethyltetrahydrofuro[3,4-d][1,3]dioxol-4-yl)methyl 4-methylbenzenesulfonate (2)

Alcohol **1** (1.14 g, 4.01 mmol, 1 EQ) was dissolved in anhydrous CH_2Cl_2 (16 mL) at rt. Pyridine (3.5 mL, 43.4 mmol, 10.3 EQ) was added into the reaction. Tosyl anhydride (2.231 g, 6.84 mmol, 1.6 EQ) was added to the reaction, after which the mixture was stirred at reflux for 2 hr. The reaction was stopped and rested without stirring at rt for 1 hour, then diluted with $CHCl_3$ (80 mL). The diluted solution was washed with 0.5 M HCl (3 x 50 mL) and saturated $NaHCO_3$ solution (60 mL), then dried over $MgSO_4$. The resulting solution was filtered and concentrated *in vacuo*. The crude product was purified with column chromatography (Hexanes:EtOAc, 1:3-1:5) to afford tosylate **2** (1.74 g, 99% yield) as a white foam. R_f (1:4 hexanes:EtOAc) = 0.51

^{1}HNMR (400 MHz, $CDCl_3$): δ 1.18 (s, 3 H), 1.38 (s, 3 H), 2.26 (s, 3 H), 4.17 (s, 3 H), 4.67 (s, 1 H), 4.87 (d, J = 6.3, 1 H), 5.60 (d, J = 7.8, 1 H), 7.17 (d, J = 8.2, 2 H), 7.61 (d, J = 8.2, 2 H)

^{13}CNMR (100.5 MHz, $CDCl_3$): δ 21.51, 25.04, 26.89, 69.74, 80.84, 84.24, 85.19, 94.91, 102.38, 114.32, 127.83, 129.82, 132.29, 143.19, 145.22, 150.30, 164.01

The ^{1}HNMR and ^{13}CNMR correspond to the literature data.[26]

C. *Azidonucleoside synthesis*

1-((3aR,4R,6R,6aR)-6-(azidomethyl)-2,2-dimethyltetrahydrofuro[3,4-d][1,3]dioxol-4-yl)pyrimidine-2,4(1H,3H)-dione (3)

Tosylate **2** (1.74 g, 3.97 mmol, 1 EQ) was dissolved in anhydrous DMF (10 mL) to which NaN$_3$ (1.35 g, 20.8 mmol, 4.9 EQ) was added. The reaction was stirred at rt for 15 minutes, then stirred at 45°C for 19 hours. Due to the formation of white sediment at the bottom of the flask, the reaction was restarted after adding more DMF (7 mL) and stirred at 40°C for 25 hours. The resulting mixture was concentrated under reduced pressure and purified via silica gel column chromatography (MeOH:CH$_2$Cl$_2$, 0-5%) to afford azide **3** (1.108 g, 90% yield) as a white foam. R$_f$ (2% MeOH:CH$_2$Cl$_2$) = 0.71

^{1}HNMR (400 MHz, CDCl$_3$): δ 1.36 (s, 3 H), 1.57 (s, 3 H), 3.63 (d, J = 4.7, 2 H), 4.24 (d, J = 4.3, 1 H), 4.84 (d, J = 5, 1 H), 5.04 (d, J = 7.2, 1 H), 5.78 (d, J = 7.8, 1 H), 5.79 (s, 1 H), 7.36 (d, J = 7.8, 1 H), 10.35 (s, 1 H)

^{13}CNMR (100.5 MHz, CDCl$_3$): δ 25.15, 27.00, 52.27, 81.49, 84.24, 85.80, 94.67, 102.68, 114.61, 142.76, 150.28, 163.94

The ^{1}HNMR and ^{13}CNMR correspond to the literature data.[26]

D. *Propargyl ether formation*

Methyl 4-(but-2-yn-1-yloxy)benzoate (4)

Commercially available methyl-4-hydroxybenzoate (1.119 g, 7.35 mmol, 1 EQ) was dissolved in anhydrous DMF (14.5 mL) at 0°C. Sodium hydride (60% mineral oil dispersion, 0.278 g, 11.6 mmol, 1.1 EQ) was added and the reaction was stirred for 1 hour at 0°C. 1-Bromo-2-butyne (0.672 mL, 7.68 mmol, 1.1 EQ) was added to the mixture

and the reaction was stirred for 19.5 hours at rt. Upon completion, the mixture was quenched with a saturated solution of NH_4Cl (15 mL) and product was extracted with EtOAc (2 x 10 mL). The combined organic layers were washed with brine (2 x 20 mL), dried over $MgSO_4$, filtered, and concentrated under reduced pressure. Silica gel column chromatography (Hexanes:EtOAc, 4:1-1:1) was used to purify ester **4** (0.63 g, 42% yield) as a white powder. R_f (3:1 hexanes:EtOAc) = 0.71

^{1}HNMR (400 MHz, $CDCl_3$): δ 1.86 (s, 3 H), 3.88 (s, 3 H), 4.70 (s, 2 H), 6.98 (d, J = 7.8, 2 H), 7.99 (d, J = 7.8, 2 H)

^{13}CNMR (100.5 MHz, $CDCl_3$): δ 3.68, 51.90, 56.52, 73.35, 84.39, 114.48, 123.10, 131.50, 161.51, 166.80

The ^{1}HNMR corresponds to the literature data.[24]

E. De-esterification of propargyl ether methyl ester

4-(But-2-yn-1-yloxy)benzoic acid (5)

Ester **4** (0.61 g, 3.0 mmol, 1 EQ) was dissolved in anhydrous THF (12 mL) at rt. KOH (1.135 g, 20.2 mmol, 6.8 EQ) was dissolved in 70% methanol (14 mL MeOH, 6 mL H_2O) to create a 1 N solution of KOH in 70% MeOH. The KOH solution was added to the reaction flask at rt, after which the reaction was stirred for 26 hours. The resulting mixture was concentrated under reduced pressure and diluted with EtOAc (150 mL), then transferred to a beaker and stirred at 0°C. The diluted solution was treated with 1 M HCl (19 mL) dropwise until the pH reached 2 when spotted onto pH paper with capillary tubes. The acidified solution was washed with brine (3 x 60 mL), filtered, dried over

$MgSO_4$, and concentrated *in vacuo* to afford benzoic acid **5** as a white crystal in its pure

form (0.54 g, 95% yield).

^{1}HNMR (400 MHz, CD_3OD): δ 1.83 (s, 3 H), 4.74 (s, 2 H), 7.03 (d, J = 9, 2 H), 7.95 (d, J

= 9, 2 H)

^{13}CNMR (100.5 MHz, CD_3OD): δ 1.63, 55.82, 73.20, 83.26, 114.16, 123.05, 131.23,

161.75, 168.26

The ^{1}HNMR corresponds to the literature data.[24]

F. THP-protected hydroxamic acid conversion

(9H-fluoren-9-yl)methyl ((2S)-1-oxo-1-(((tetrahydro-2H-pyran-2-yl)oxy)amino)pent-4-yn-2-yl)carbamate (6)

Commercially available Fmoc-L-Propargylglycine (198 mg, 0.59 mmol, 1 EQ) was

dissolved in anhydrous CH_2Cl_2 (2 mL) at 0°C. THP-O-NH_2 (79 mg, 0.67 mmol, 1.1 EQ)

was added at 0°C. In a separate flask, DCC (142 mg, 0.69 mmol, 1.1 EQ) was dissolved

with anhydrous CH_2Cl_2 (2 mL) under Ar. The DCC solution was added dropwise to the

Fmoc solution at 0°C, then the mixture stirred for 10 minutes at 0°C. The reaction was

warmed to rt and stirred for 21 hours. The solution was filtered through cotton, during

which the reaction flask and filter were rinsed with CH_2Cl_2 and CH_3CN. Once

concentrated under reduced pressure, the product was purified with silica gel column

chromatography (MeOH:CH_2Cl_2, 10%) to afford the THP-protected hydroxamic acid **6**

(265 mg, 103% yield) as a white powder. R_f (10% MeOH:CH_2Cl_2) = 0.88, visualized

with potassium permanganate stain

^{1}HNMR (400 MHz, CDCl$_3$): δ 1.54 (m, 3 H), 1.74 (m, 2 H), 2.06 (s, 1 H), 2.68 (d, 2 H), 3.52 (d, 1 H), 3.89 (t, 1 H), 4.18 (t, 1 H), 4.33 (t, 1 H), 4.40 (d, 2 H), 4.95 (t, 1 H), 5.98 (d, 1 H), 7.29 (m, 2 H), 7.38 (m, 2 H), 7.55 (m, 2 H), 7.73 (m, 2 H), 9.95 (s, 1 H)

The ^{1}HNMR corresponds to the literature data.[14]

G. Coupling of THP-Protected Hydroxamic Acid and Phenyl Propargyl Ether Benzoic Acid

4-(But-2-yn-1-yloxy)-N-((2S)-1-oxo-1-((((tetrahydro-2H-pyran-2-yl)oxy)amino)pent-4-yn-2-yl)benzamide (7)

Protected hydroxamic acid **6** (262 mg, 0.60 mmol, 1 EQ) was dissolved in anhydrous CH$_2$Cl$_2$ (2.5 mL) at 0°C and treated dropwise with piperidine (20% in DMF, 1 mL). The reaction was stirred for 11 minutes at 0°C, with reaction progress checked every 5 minutes by TLC and ninhydrin staining. The product was reduced under pressure and used without purification. Benzoic acid **5** (338 mg, 1.78 mmol, 3 EQ) was transferred to the reaction flask containing the protected hydroxamic acid **6** with anhydrous CH$_2$Cl$_2$ (7 mL), dissolving both compounds. HATU (730 mg, 1.92 mmol, 3.2 EQ) and DIPEA (0.95 mL, 5.3 mmol, 9 EQ) were added and the reaction was stirred for 4 hours at rt. The mixture was concentrated under reduced pressure. Purification by column chromatography (Hexanes:EtOAc, 1:1-2:1) was attempted, but most spots reported were byproducts rather than the pure product **7**. No product was obtained.

H. Methyl ester protection

Methyl (S)-2-((((9H-fluoren-9-yl)methoxy)carbonyl)amino)pent-4-ynoate (8)

Commercially available Fmoc-L-propargylglycine (289 mg, 0.91 mmol, 1 EQ) was

dissolved in MeOH at 0°C. SOCl$_2$ (0.15 mL, 2.1 mmol, 2 EQ) was added dropwise at

0°C after which the reaction was heated to 60°C and stirred for 4 hours. As the reaction

progressed, a white mass formed on top of a dark green solution, so anhydrous CH$_2$Cl$_2$ (1

mL) was added to improve solubility. The crude mixture was concentrated under reduced

pressure to form the glassy crude product. Silica gel column chromatography

(MeOH:CH$_2$Cl$_2$, 2%) afforded methyl ester **8** (319 mg, 100% yield) as a white powder.

R$_f$ (2% MeOH:CH$_2$Cl$_2$) = 0.92

^{1}HNMR (400 MHz, CDCl$_3$): δ 2.07 (s, 1 H), 2.79 (s, 2 H), 3.80 (s, 3 H), 4.24 (t, J =

7(x2), 1 H), 4.40 (d, J = 7, 2 H), 4.55 (t, J = 4(x2), 1 H), 5.67 (d, J = 7.4, 1 H), 7.31 (t, J =

7(x2), 2 H), 7.40 (t, J = 7.4(x2), 2 H), 7.61 (d, J = 7, 2 H), 7.76 (d, J = 7.4, 2 H)

^{13}CNMR (100.5 MHz, CDCl$_3$): δ 22.76, 47.11, 52.35, 52.82, 67.25, 71.87, 78.26, 120.00,

125.11, 127.08, 127.74, 141.29, 143.71, 143.80, 155.61, 170.77

The ^{1}HNMR and ^{13}CNMR correspond to the literature data.[27]

I. Methyl ester and benzoic acid coupling with HATU

Methyl (S)-2-(4-(but-2-yn-1-yloxy)benzamido)pent-4-ynoate (9)

Methyl ester **8** (345 mg, 0.99 mmol, 1 EQ) was dissolved in anhydrous CH$_2$Cl$_2$ (2.5 mL)

at 0°C and treated dropwise with piperidine (20% in DMF, 1 mL). Reaction progress was

monitored with a ninhydrin stain, with complete Fmoc removal occurring after 18

minutes. The mixture was reduced under pressure and used without further purification.[14]

Benzoic acid **5** (250 mg, 1.31 mmol, 1.51 EQ) was added to the deprotected methyl ester

with anhydrous CH_2Cl_2 (8 mL) and dissolved at rt. HATU (597 mg, 1.57 mmol, 1.6 EQ)

and DIPEA (0.80 mL, 4.6 mmol, 4.5 EQ) were added and the reaction was stirred for 24

hours at rt. The mixture was reduced under pressure and purified via column

chromatography (Hexanes:EtOAc, 4:1-1:1) to produce alkyne **9** (240 mg, 81% yield) as a

white solid. R_f (3:1 hexanes:EtOAc) = 0.28.

^{1}HNMR (400 MHz, $CDCl_3$): δ 1.86 (s, 3 H), 2.07 (s, 1 H), 2.89 (ddd, J = 8.1, 4.8, 2.7, 2

H), 3.82 (s, 3 H), 4.70 (d, J = 2, 2 H), 4.94 (dt, J = 7.8, 4.7(x2), 1 H), 6.94 (d, J = 7.4, 1

H), 7.01 (d, J = 9, 2 H), 7.81 (d, J = 9, 2 H)

^{13}CNMR (100.5 MHz, $CDCl_3$): δ 3.64, 22.57, 50.94, 52.83, 56.47, 71.67, 73.37, 78.55,

84.34, 114.70, 126.41, 128.91, 160.65, 166.39, 171.04

J. Methyl ester and benzoic acid coupling with EDC

Methyl (S)-2-(4-(but-2-yn-1-yloxy)benzamido)pent-4-ynoate (9)

Methyl ester **8** (290 mg, 0.83 mmol, 1 EQ) was dissolved in anhydrous CH_2Cl_2 (2.5 mL)

at 0°C and treated dropwise with piperidine (20% in DMF, 1 mL). Reaction progress was

monitored with a ninhydrin stain, with complete Fmoc removal occurring after 21

minutes. The mixture was reduced under pressure and used without further purification.[14]

Benzoic acid **5** (238 mg, 1.25 mmol, 1.51 EQ) was added to the deprotected methyl ester

with anhydrous CH_2Cl_2 (8 mL) and stirred at rt for 30 minutes. EDC·HCl (238 mg, 1.24

mmol, 1.4 EQ) and HOBt (219 mg, 1.43 mmol, 1.4 EQ) were added at 0°C and the

reaction was stirred for 15 minutes. DIPEA (0.5 mL, 3 mmol, 4.5 EQ) was added

dropwise at 0°C after which the mixture was stirred for 20 minutes. The reaction was

warmed to rt and stirred for 24 hours. The mixture was diluted with CH_2Cl_2 (20 mL) and washed with 1.6 M citric acid (30 mL), saturated $NaHCO_3$ solution (30 mL), and brine (30 mL). The organic layer was dried over Na_2SO_4, filtered, and concentrated *in vacuo*. Purification by column chromatography (Hexanes:EtOAc, 4:1-1:1) afforded alkyne **9** (142 mg, 57% yield) as a white solid. R_f (2:1 hexanes:EtOAc) = 0.33.

^{1}HNMR (400 MHz, $CDCl_3$): δ 1.38 (s, 3 H), 2.04 (d, 1 H), 2.86 (m, 2 H), 3.80 (s, 3 H), 4.68 (s, 2 H), 4.19 (m, 1 H), 6.98 (m, 2 H), 7.78 (m, 2 H)

^{13}CNMR (100.5 MHz, $CDCl_3$): δ 3.64, 22.57, 50.94, 52.83, 56.47, 71.67, 73.37, 78.55, 84.33, 114.70, 126.41, 128.90, 160.64, 166.38, 171.03

K. *Hydroxamic acid conversion*

(S)-4-(But-2-yn-1-yloxy)-N-(1-(hydroxyamino)-1-oxopent-4-yn-2-yl)benzamide (10)

A solution of NH_2OH (50% in H_2O, 0.80 mL, 26 mmol, 55 EQ) in MeOH (3 mL) was prepared and its pH tested to be no greater than 8. Alkyne **9** (136 mg, 0.45 mmol, 1 EQ) was dissolved in the NH_2OH & MeOH solution at rt and stirred for 22 hours. The solution was concentrated under reduced pressure to afford the pure hydroxamic acid **10** (137 mg, 100% yield) as a white solid.

^{1}HNMR (400 MHz, DMSO): δ 1.81 (s, 3 H), 2.59 (m, 2 H), 2.83 (s, 3 H), 4.49 (m, 1 H), 4.79 (s, 2 H), 7.01 (m, 2 H), 7.84 (m, 2 H), 8.48 (d, 1 H), 8.93 (d, 1 H), 10.79 (s, 1 H)

^{13}CNMR (100.5 MHz, DMSO): δ 3.59, 22.02, 50.67, 56.42, 73.25, 74.84, 81.32, 84.29, 114.62, 126.97, 129.78, 160.20, 166.02, 167.24

L. Triazole formation via CuAAC

4-(But-2-yn-1-yloxy)-N-((S)-3-(1-(((3aR,4R,6R,6aR)-6-(2,4-dioxo-3,4-dihydropyrimidin-1(2H)-yl)-2,2-dimethyltetrahydrofuro[3,4-d][1,3]dioxol-4-yl)methyl)-1H-1,2,3-triazol-4-yl)-1-(hydroxyamino)-1-oxopropan-2-yl)benzamide (11)

Alkyne **10** (190 mg, 0.63 mmol, 1 EQ) was dissolved in CH_3CN (3 mL). In a separate flask, azide **3** (200 mg, 0.65 mmol, 1 EQ) was dissolved in anhydrous CH_3CN (1.5 mL) and transferred into the flask containing alkyne **9**. H_2O (1.2 mL) and Cu powder (18 mg, 0.28 mmol, 0.36 EQ) were added at rt. The reaction was sonicated for 10 minutes, then heated to 35°C and stirred for 23.5 hours. The resulting mixture was concentrated under reduced pressure. Column chromatography (MeOH:CH_2Cl_2, 5-10%) afforded the desired product **11** (150 mg, 39% yield) as an off-white solid. R_f (8% MeOH:CH_2Cl_2) = 0.33

^{1}HNMR (400 MHz, DMSO): δ 1.23 (s, 3 H), 1.41 (s, 3 H), 1.81 (s, 3 H), 3.06 (d, J = 7, 2 H), 4.26 (m, 1 H), 4.58 (d, J = 8.3, 2 H), 4.65 (d, J = 4.3, 1 H), 4.69 (d, J = 4.7, 1 H), 4.78 (s, 3 H), 5.03 (d, J = 6.3, 1 H), 5.62 (d, J = 7.8, 1 H), 5.75 (s, 1 H), 6.97 (d, J = 8.6, 2 H), 7.60 (d, J = 8.2, 1 H), 7.78 (d, J = 8.6, 2 H), 7.80 (s, 1 H), 8.46 (d, J = 8.2, 1 H), 8.86 (s, 1 H)

^{13}CNMR (100.5 MHz, DMSO): δ 3.59, 25.51, 27.26, 51.41, 56.39, 74.85, 81.58, 83.93, 84.26, 85.56, 93.23, 102.38, 113.91, 114.55, 123.84, 127.13, 129.68, 143.72, 143.85, 150.74, 160.12, 163.70, 166.15, 168.22

M. Ketal Deprotection

4-(but-2-yn-1-yloxy)-N-((S)-3-(1-(((2R,3S,4R,5R)-5-(2,4-dioxo-3,4-dihydropyrimidin-1(2H)-yl)-3,4-dihydroxytetrahydrofuran-2-yl)methyl)-1H-1,2,3-triazol-4-yl)-1-(hydroxyamino)-1-oxopropan-2-yl)benzamide (DP-001)

Hydroxamic acid **11** (78 mg, 0.13 mmol, 1 EQ) was dissolved in CH_2Cl_2 (5 mL) at 0°C. DI water (0.2 mL) was added dropwise at 0°C. TFA (0.8 mL, 0.10 mmol, 1 EQ) was added dropwise at 0°C. The reaction was sealed with a glass stopper and stirred for 20 hours. The mixture was transferred to a conical flask with 1:1 CH_2Cl_2:MeOH and concentrated under reduced pressure to a brown foam, then treated with 3 drops of MeOH for solubility. The product was precipitated out with diethyl ether (59 mg, 81% yield) as an off-white solid.

^{1}HNMR (400 MHz, DMSO): δ 1.82 (s, 3 H), 3.30 (s, 1 H), 4.00 (s, 2 H), 4.09 (d, J = 4.7, 1 H), 4.17 (s, 1 H), 4.67 (m, 1 H), 4.72 (s, 2 H), 4.79 (s, 2 H), 5.66 (s, 2 H), 6.99 (d, J = 8.2, 2 H), 7.37 (m, 1 H), 7.75 (d, J = 7.8, 2 H), 7.82 (s, 1 H)

^{13}CNMR (100.5 MHz, DMSO): δ 3.05, 15.38, 29.00, 52.35, 57.17, 66.85, 71.72, 74.12, 74.68, 82.83, 92.90, 102.98, 115.58, 127.35, 130.13, 130.23, 142.97, 143.09, 151.93, 162.17, 165.92, 169.34, 169.51

Results & Discussion

A. Analog Design

Previous computational studies done by our lab group showed strong inhibitory activity by nucleoside-containing analogs in the LpxC active site.[14] **SA-002**, which did not contain a hydrophobic tail, had the most negative interaction energy at -710 kcal/mol in a solvated model.[14] However, as many key human enzymes such as matrix metalloproteinases and zinc-dependent histone deacetylases contain Zn^{2+} ions in their active sites, a hydrophobic tail must be included to provide LpxC specificity. Additionally, the incorporation of a tail moiety allows for us to further modulate the lipophilicity and solubility of the compounds which is seen in calculated log P values (Table 2). **SA-002**, which does not contain a hydrophobic tail, has the most negative Log P value, indicating that it is the most polar. **CE-002**, **DP-001**, and **GL-001** have increasingly positive log P values that correlate with their increased lipophilicity.

Table 2: Log P Values of Nucleoside Analogs

Molecule	Log P
SA-002	-3.52
GL-001	-0.01
DP-001	-1
CE-002	-1.69

*values taken from ChemDraw Professional 15.1

While prior hydrophobic regions developed by the Peterson lab contained simple phenyl and biphenyl tails (**CE-003** and **GL-001**), the phenyl propargyl ether tail developed by the Piizi group showed good active site binding and strong LpxC inhibitory

activity.[24] Due to the *in vitro* success of the phenyl propargyl ether tail, it was incorporated into the inhibitors as a hydrophobic region attached to both nucleoside and non-nucleoside analogs.

B. Optimization of Tosylation Reaction

Synthesis of the azidonucleoside (Scheme 1) began with a ketal protection of commercially available uridine to produce alcohol **1** with a yield of 96% yield.[25] Alcohol **1** underwent tosylation to form tosylate **2** in a 99% yield.[26] The tosyl group of **2** was replaced with an azide, affording azide **3** in a 90% yield.[26] The most difficult reaction in the azidonucleoside synthesis is the tosylation of the protected nucleoside. Though the literature showed yields of 98%, previous members of the lab could not produce yields above 67%. This is likely caused by the difficult aqueous workup, which can form an emulsification layer that prevents good separation. Measures taken to optimize tosylation include scaling down and resting the reaction at room temperature for an extra hour upon completion before beginning the aqueous workup. The procedure of the aqueous work up involves three washes with 0.5M HCl and one wash with saturated sodium bicarbonate solution. In the event an emulsification layer formed, brine was added into the separation flask in order to produce a more ionic solution and resolve the emulsification layer. In literature, the tosylate was purified via silica gel column chromatography in chloroform:methanol.[26] Conditions were changed to Hexanes:EtOAc on a gradient of 1:3 to 1:5 so as to accelerate the product's elution through the column. Under these conditions, the yield was improved to 99%, which is comparable to the literature values.

The tosylated product **2** was then converted to azide **3**, which would be clicked together with the alkyne via CuAAC.

Scheme 1
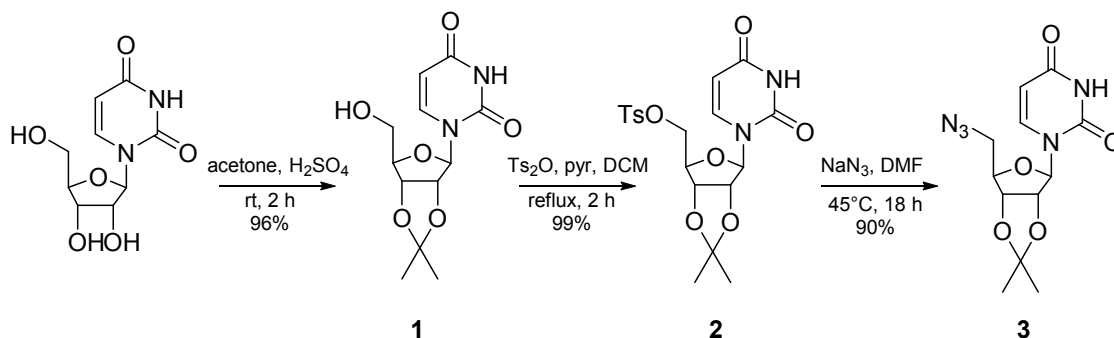
C. Propargyl Ether Benzoic Acid Synthesis

The propargyl ether benzoic acid derivative was synthesized as outlined in Scheme 2, which was derived from Piizi et al.[24] Methyl-4-hydroxybenzoate underwent standard Williamson ether synthesis to form ester **4** with a yield of 42%.[24] Ester **4** was converted to benzoic acid **5** in a 95% yield.[24] While the de-esterification reaction yield was similar to the 96% yield found in literature, the ether synthesis yield was lower than the literature yield of 59%. This low product yield may have been caused by many factors, including inactive sodium hydride or the 0°C temperature at which the reaction began. Further optimization may be achieved by rinsing the sodium hydride with hexanes and transferring the pure sodium hydride via cannula into the reaction flask. Additionally, using new sodium hydride may improve ether synthesis yields.

While the de-esterification reaction did have a high yield of 96%, great care had to be taken to properly acidify the compound. Following treatment with potassium hydroxide and methanol in THF, benzoate **4** was acidified with 1M HCl at 0°C to pH 2. The

acidified solution was washed with brine and dried over magnesium sulfate. In some

cases, the compound was reacidified to insure complete formation of the benzoic acid and

transfer the compound into the organic layer. Despite using magnesium sulfate to dry the

compound, a significant water signal was observed in the spectra taken of the final

benzoic acid **5**, which may have complicated the subsequent coupling steps.

Scheme 2
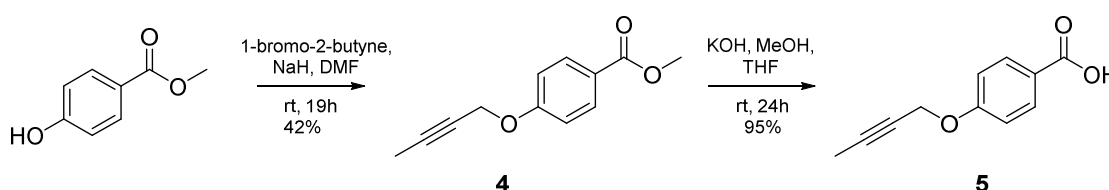
D. Exploration of Amide Coupling Methods: THP-Protected Hydroxamic Acid

For all other analogs in the Peterson library, a THP-protected hydroxamic acid was

coupled with the corresponding benzoic acid to result in the alkyne half of the

molecule.[14] This alkyne would undergo CuAAC, or click chemistry, with

azidonucleoside **3** to form a triazole linker between the two portions of the molecule. The

initial approach for the synthesis of **DP-001** was to utilize this technique as well (Scheme

3). Commercially available Fmoc-L-propargylglycine was converted to THP-protected

hydroxamic acid **6** with a 78% yield.[28] Prior to amide coupling, the Fmoc group of alkyne

6 was removed with piperidine.[14] The resulting alkyne was coupled using HATU to

benzoic acid derivative **5**.[24] Despite success in literature, the HATU coupling procedure

did not result in alkyne **7** formation. This may be in part due to water which could not be

completely removed from benzoic acid **5**, effectively preventing HATU coupling activity.

Improper acidification of the benzoic acid derivative may have resulted in less benzoic

acid in solution, thus preventing the necessary interactions for product formation.

Additionally, molar proportions were miscalculated, leaving an excess of benzoic acid **5**

which made isolating any product very difficult.

Scheme 3
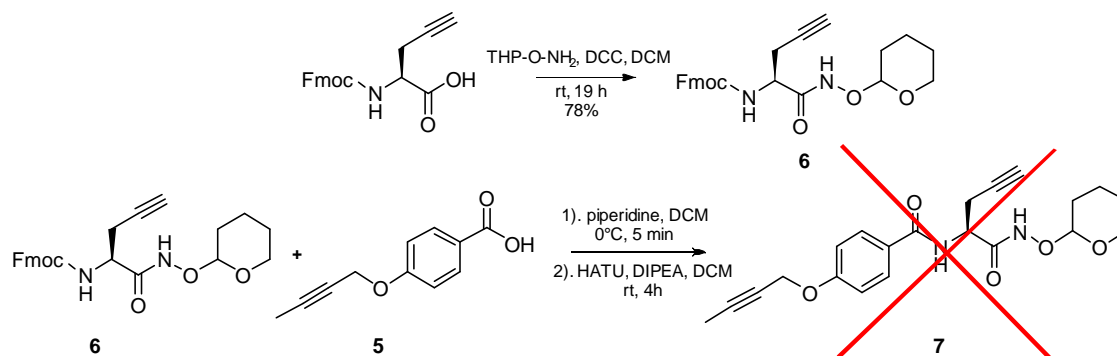
E. Methyl Ester Protection & Coupling

As the THP-protected hydroxamic acid **7** did not couple with benzoic acid derivative

5, a new synthetic design was created with the aim of affording the coupled alkyne

(Scheme 4). A survey of other LpxC inhibitor synthetic procedures found a common

approach involving a methyl ester that could later be converted to a hydroxamic acid,

often in the last step of synthesis.[24, 29] In the interests of pursuing this method, Fmoc-L-

propargylglycine was esterified using thionyl chloride to form methyl ester **8** in a 100%

yield.[27] The Fmoc protecting group of methyl ester **8** was removed with piperidine prior

to coupling with benzoic acid **5** to afford alkyne **9**. Various coupling agents were

explored to synthesize alkyne **9**, including EDC and HATU. The EDC procedure had

been previously used by our lab to synthesize **CE-001**, and successfully produced alkyne

9 in a 57% yield.[14] The HATU coupling procedure was even more successful, with

alkyne **9** afforded in an 81% yield, improving upon the literature yield of 51%.[24]

Scheme 4
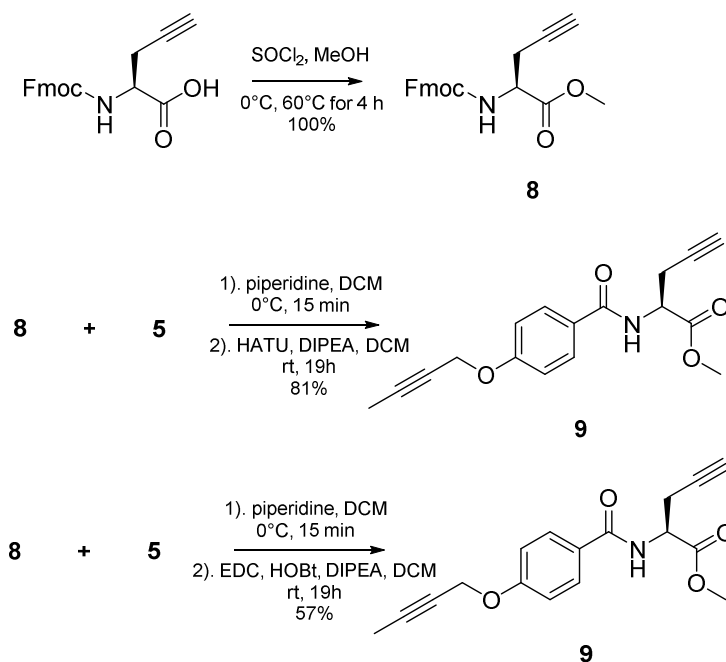
Though HATU was a more successful agent than EDC, the cost of HATU is quite

high in comparison. HATU is also more sensitive to water in the reaction, and may not

couple if any residual water remains. As such, EDC may be the preferred method for the

amide coupling procedure. Another coupling agent option is HBTU, as it has the

functionality of HATU at a more reasonable cost.[30]

F. Hydroxamic Acid Conversion

The coupled methyl ester **9** was converted to hydroxamic acid **10** through treatment

with aqueous hydroxylamine quantitatively (Scheme 5).[24] This step afforded **DP-002**, the

non-nucleoside analog with the propargyl ether tail. Unlike other literature examples,

which use highly basic solutions to achieve hydroxamate conversion of methyl esters, the

sensitivity of the α-proton to removal by a base necessitated less basic conditions so as not to risk racemization. Hydroxylamine (50% in water) was diluted with methanol until the pH registered close to 8. Methyl ester **9** was dissolved in this solution at room temperature and stirred for 22 hours, after which thin-layer chromatography (TLC) confirmed that only hydroxamic acid **10** was present. Synthesis of alkyne **DP-002** was confirmed through ^{1}HNMR and ^{13}CNMR, as spectra contained peaks that correspond to the hydroxamic acid group. **DP-002** was fully synthesized in 7 steps with an overall yield of 28%.

In the current synthetic procedure, the hydroxamic acid conversion precedes the CuAAC reaction as the uracil group on the nucleoside may be susceptible to basic degradation in hydroxylamine. While the hydroxamic conversion successfully afforded **DP-002**, the nucleoside analog **DP-001** was more synthetically challenging.

Scheme 5

9   10
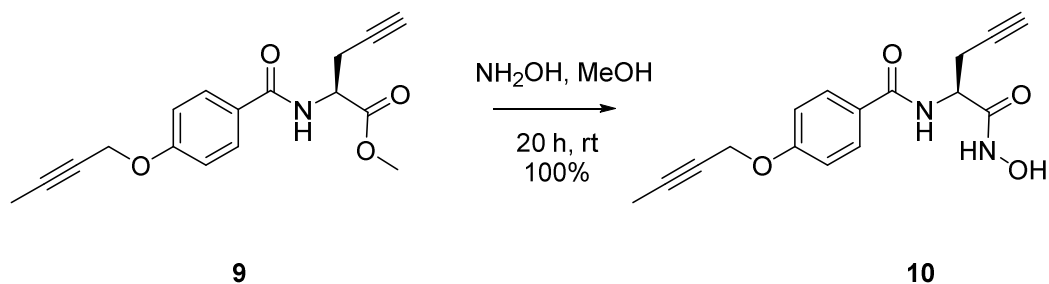
G. Click Chemistry

Copper-catalyzed azide-alkyne cycloaddition (CuAAC), or click chemistry, was used previously in our lab to synthesize triazole-linked compounds **SA-002**, **GL-001**, and **CE-003** with yields from 54-77%.[14] Azide **3** and alkyne **10** were dissolved in acetonitrile,

after which Cu powder was added to the reaction flask. Following sonication, the reaction

ran for 23.5 hours at 32°C to afford **11** in 39% yield, which was significantly lower than

previous yields of other nucleoside analogs (Scheme 6).[14] This reduced yield may be in

part due to failure to run the reaction to completion. As this was the first attempt at using

CuAAC on a compound with an exposed hydroxamic acid, it is possible that the reaction

needed more than 24 hours to reach completion. Any future CuAAC reactions should be

monitored by TLC to confirm product formation and reaction completion.

Scheme 6
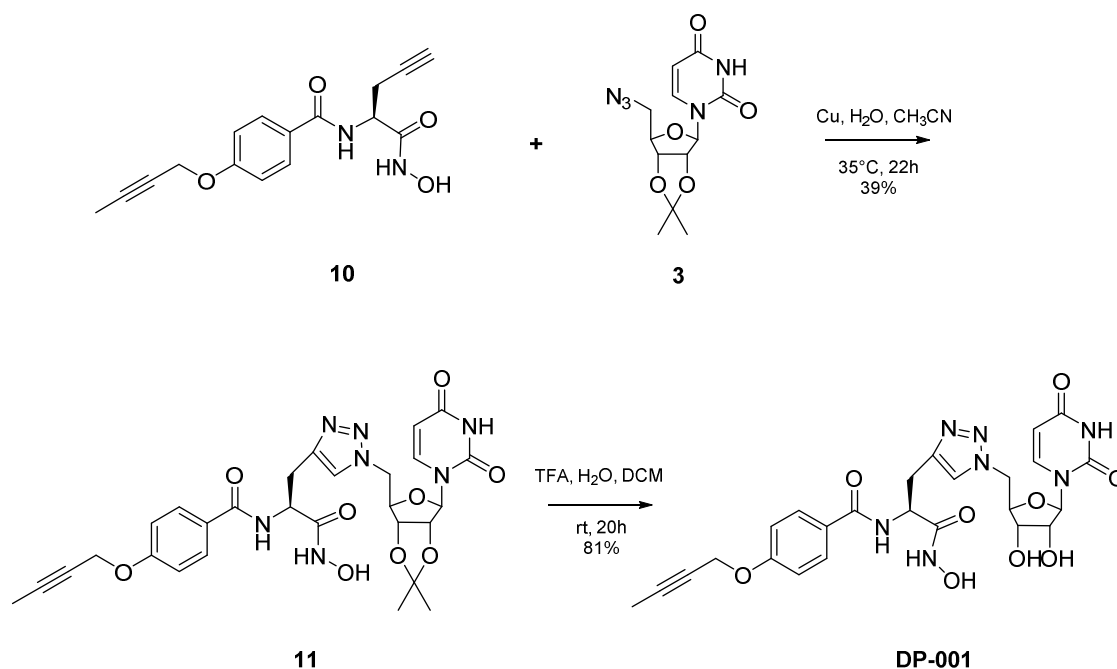
The exposed hydroxamic acid may also be causing some complications during this

reaction. Hydroxamates are capable of binding to metallic ions with a 2+ charge.[16] While

other CuAAC procedures use Cu (II) salts, our use of Cu powder results in only Cu^+

formation, thus not interfering with the hydroxamic acid. However, the column needed

for purification allows a chance for the hydroxamic acid to interact with and adhere to

highly polar silica gel, causing loss of product.

Upon purification, compound **11** was treated with trifluoroacetic acid at 0°C in order to remove the ketal protecting group. After the reaction ran for 20 hours, the mixture was concentrated under reduced pressure. Purification was achieved through precipitation with diethyl ether. Prior to precipitation, a small amount of methanol was added to the flask to improve solubility. **DP-001** was isolated in a 81% yield, which was lower than literature yields of 65-70% (Scheme 6).[14] Synthesis was confirmed with ^{1}HNMR and ^{13}CNMR. **DP-001** was fully synthesized in 9 steps with an overall yield of 9%.

Conclusions

Inhibition of LpxC is a promising method of antibacterial treatment that may be useful in against multidrug resistant bacteria. The most effective inhibitors found in literature share a hydroxamate to bind to the Zn^{2+} ion and an aromatic tail that can bind specifically in the hydrophobic passage. Of these inhibitors, none have specifically targeted the nucleoside binding pocket proximal to the Zn^{2+} ion. The development of nucleoside-based analogs that mimic the natural substrate of LpxC provide insight into key active site interactions. **DP-001** and **DP-002**, which contain a phenyl propargyl ether tail attached to the triazole-linked hydroxamate and nucleoside, have been added to the Peterson library as potential LpxC inhibitors. **DP-002** has been fully synthesized in 7 steps with an overall yield of 28%. **DP-001** was synthesized in 9 steps with an overall yield of 9%. Computational and experimental results with the newly developed inhibitors will provide insight into how to successfully inhibit LpxC activity, and will drive design and synthesis of additional inhibitors.

References

1.   Ventola, C. L., The Antibiotic Resistance Crisis: Part 1: Causes and Threats. *Pharmacy and Therapeutics* **2015,** *40* (4), 277-283.

2.   Exner, M.; Bhattacharya, S.; Christiansen, B.; Gebel, J.; Goroncy-Bermes, P.; Hartemann, P.; Heeg, P.; Ilschner, C.; Kramer, A.; Larson, E.; Merkens, W.; Mielke, M.; Oltmanns, P.; Ross, B.; Rotter, M.; Schmithausen, R. M.; Sonntag, H.-G.; Trautmann, M., Antibiotic resistance: What is so special about multidrug-resistant Gram-negative bacteria? *GMS Hygiene and Infection Control* **2017,** *12*, Doc05.

3.   CDC Antibiotic resistance threats in the United States, 2013. (accessed April 11, 2018).

4.   Weiner, L. M.; Webb, A. K.; Limbago, B.; Dudeck, M. A.; Patel, J.; Kallen, A. J.; Edwards, J. R.; Sievert, D. M., Antimicrobial-Resistant Pathogens Associated With Healthcare-Associated Infections: Summary of Data Reported to the National Healthcare Safety Network at the Centers for Disease Control and Prevention, 2011–2014. *Infection Control & Hospital Epidemiology* **2016,** *37* (11), 1288-1301.

5.   Neidell, M. J.; Cohen, B.; Furuya, Y.; Hill, J.; Jeon, C. Y.; Glied, S.; Larson, E. L., Costs of Healthcare- and Community-Associated Infections With Antimicrobial-Resistant Versus Antimicrobial-Susceptible Organisms. *Clin. Infect. Dis.* **2012,** *55* (6), 807-815.

6.   Epstein, L.; Dantes, R.; Magill, S.; Fiore, A., *Varying Estimates of Sepsis Mortality Using Death Certificates and Administrative Codes - United States, 1999-2014*. 2016; Vol. 65, p 342-345.

7.   Miller, S. I., Antibiotic Resistance and Regulation of the Gram-Negative Bacterial Outer Membrane Barrier by Host Innate Immune Molecules. *mBio* **2016,** *7* (5).

8.   Brown, L.; Wolf, J. M.; Prados-Rosales, R.; Casadevall, A., Through the wall: extracellular vesicles in Gram-positive bacteria, mycobacteria and fungi. *Nature reviews. Microbiology* **2015,** *13* (10), 620-630.

9.   Zhang, G.; Meredith, T. C.; Kahne, D., On the Essentiality of Lipopolysaccharide to Gram-Negative Bacteria. *Curr. Opin. Microbiol.* **2013,** *16* (6), 779-785.

10.   Blair, J. M. A.; Webber, M. A.; Baylay, A. J.; Ogbolu, D. O.; Piddock, L. J. V., Molecular mechanisms of antibiotic resistance. *Nature Reviews Microbiology* **2014,** *13*, 42.

11.   Ramachandran, G., Gram-positive and gram-negative bacterial toxins in sepsis: A brief review. *Virulence* **2014,** *5* (1), 213-218.

12.   Steimle, A.; Autenrieth, I. B.; Frick, J.-S., Structure and function: Lipid A modifications in commensals and pathogens. *Int. J. Med. Microbiol.* **2016,** *306* (5), 290-301.

13.   Barb, A. W.; Zhou, P., Mechanism and inhibition of LpxC: An essential zinc-dependent deacetylase of bacterial lipid a synthesis. *Curr. Pharm. Biotechnol.* **2008,** *9* (1), 9-15.

14.   Malkowski, S.; Dishuck, C.; Lamanilao, G.; Embry, C.; Grubb, C.; Cafiero, M.; Peterson, L., Design, Modeling and Synthesis of 1,2,3-Triazole-Linked Nucleoside-Amino Acid Conjugates as Potential Antibacterial Agents. *Molecules* **2017,** *22* (10), 1682.

15.   Zuo, K.; Liang, L.; Du, W.; Sun, X.; Liu, W.; Gou, X.; Wan, H.; Hu, J., 3D-QSAR, Molecular Docking and Molecular Dynamics Simulation of Pseudomonas aeruginosa LpxC Inhibitors. *International Journal of Molecular Sciences* **2017,** *18* (5).

16.   Dewar, J. C.; Thakur, A. S.; Brennessel, W. W.; Cafiero, M.; Peterson, L. W.; Eckenhoff, W. T., Simple zinc complex to model substrate binding to zinc enzymes. *Inorg. Chim. Acta* **2018,** *473*, 15-19.

17.   Tangherlini, G.; Torregrossa, T.; Agoglitta, O.; Köhler, J.; Melesina, J.; Sippl, W.; Holl, R., Synthesis and biological evaluation of enantiomerically pure glyceric acid derivatives as LpxC inhibitors. *Biorg. Med. Chem.* **2016,** *24* (5), 1032-1044.

18.   Lee, C.-J.; Liang, X.; Wu, Q.; Najeeb, J.; Zhao, J.; Gopalaswamy, R.; Titecat, M.; Sebbane, F.; Lemaitre, N.; Toone, E. J.; Zhou, P., Drug design from the cryptic inhibitor envelope. *Nature Communications* **2016,** *7*, 10638.

19.   Montgomery, J. I.; Brown, M. F.; Reilly, U.; Price, L. M.; Abramite, J. A.; Arcari, J.; Barham, R.; Che, Y.; Chen, J. M.; Chung, S. W.; Collantes, E. M.; Desbonnet, C.; Doroski, M.; Doty, J.; Engtrakul, J. J.; Harris, T. M.; Huband, M.; Knafels, J. D.; Leach, K. L.; Liu, S.; Marfat, A.; McAllister, L.; McElroy, E.; Menard, C. A.; Mitton-Fry, M.; Mullins, L.; Noe, M. C.; O'Donnell, J.; Oliver, R.; Penzien, J.; Plummer, M.; Shanmugasundaram, V.; Thoma, C.; Tomaras, A. P.; Uccello, D. P.; Vaz, A.; Wishka, D. G., Pyridone Methylsulfone Hydroxamate LpxC Inhibitors for the Treatment of Serious Gram-Negative Infections. *J. Med. Chem.* **2012,** *55* (4), 1662-1670.

20.   Tomaras, A. P.; McPherson, C. J.; Kuhn, M.; Carifa, A.; Mullins, L.; George, D.; Desbonnet, C.; Eidem, T. M.; Montgomery, J. I.; Brown, M. F.; Reilly, U.; Miller, A. A.; O'Donnell, J. P., LpxC Inhibitors as New Antibacterial Agents and Tools for Studying

Regulation of Lipid A Biosynthesis in Gram-Negative Pathogens. *mBio* **2014,** *5* (5), e01551-14.

21. Titecat, M.; Liang, X.; Lee, C.-J.; Charlet, A.; Hocquet, D.; Lambert, T.; Pagès, J.-M.; Courcol, R.; Sebbane, F.; Toone, E. J.; Zhou, P.; Lemaitre, N., High susceptibility of MDR and XDR Gram-negative pathogens to biphenyl-diacetylene-based difluoromethyl-allo-threonyl-hydroxamate LpxC inhibitors. *J. Antimicrob. Chemother.* **2016,** *71* (10), 2874-2882.

22. Lee, C.-J.; Liang, X.; Chen, X.; Zeng, D.; Joo, S. H.; Chung, H. S.; Barb, A. W.; Swanson, S. M.; Nicholas, R. A.; Li, Y.; Toone, E. J.; Raetz, C. R. H.; Zhou, P., Species-Specific and Inhibitor-Dependent Conformations of LpxC: Implications for Antibiotic Design. *Chem. Biol.* **2011,** *18* (1), 38-47.

23. Liang, X.; Lee, C.-J.; Chen, X.; Chung, H. S.; Zeng, D.; Raetz, C. R. H.; Li, Y.; Zhou, P.; Toone, E. J., Syntheses, structures and antibiotic activities of LpxC inhibitors based on the diacetylene scaffold. *Biorg. Med. Chem.* **2011,** *19* (2), 852-860.

24. Piizzi, G.; Parker, D. T.; Peng, Y.; Dobler, M.; Patnaik, A.; Wattanasin, S.; Liu, E.; Lenoir, F.; Nunez, J.; Kerrigan, J.; McKenney, D.; Osborne, C.; Yu, D.; Lanieri, L.; Bojkovic, J.; Dzink-Fox, J.; Lilly, M.-D.; Sprague, E. R.; Lu, Y.; Wang, H.; Ranjitkar, S.; Xie, L.; Wang, B.; Glick, M.; Hamann, L. G.; Tommasi, R.; Yang, X.; Dean, C. R., Design, Synthesis, and Properties of a Potent Inhibitor of Pseudomonas aeruginosa Deacetylase LpxC. *J. Med. Chem.* **2017,** *60* (12), 5002-5014.

25. Bello, A. M.; Poduch, E.; Fujihashi, M.; Amani, M.; Li, Y.; Crandall, I.; Hui, R.; Lee, P. I.; Kain, K. C.; Pai, E. F.; Kotra, L. P., A Potent, Covalent Inhibitor of Orotidine

5'-Monophosphate Decarboxylase with Antimalarial Activity. *J. Med. Chem.* **2007,** *50* (5), 915-921.

26.   Winans, K. A.; Bertozzi, C. R., An Inhibitor of the Human UDP-GlcNAc 4-Epimerase Identified from a Uridine-Based Library. A Strategy to Inhibit O-Linked Glycosylation. *Chem. Biol.* **2002,** *9* (1), 113-129.

27.   Ourailidou, M. E.; Lenoci, A.; Zwergel, C.; Rotili, D.; Mai, A.; Dekker, F. J., Towards the development of activity-based probes for detection of lysine-specific demethylase-1 activity. *Biorg. Med. Chem.* **2017,** *25* (3), 847-856.

28.   Suzuki, T.; Ota, Y.; Ri, M.; Bando, M.; Gotoh, A.; Itoh, Y.; Tsumoto, H.; Tatum, P. R.; Mizukami, T.; Nakagawa, H.; Iida, S.; Ueda, R.; Shirahige, K.; Miyata, N., Rapid Discovery of Highly Potent and Selective Inhibitors of Histone Deacetylase 8 Using Click Chemistry to Generate Candidate Libraries. *J. Med. Chem.* **2012,** *55* (22), 9562-9575.

29.   Liang, X.; Gopalaswamy, R.; Navas, F.; Toone, E. J.; Zhou, P., A Scalable Synthesis of the Difluoromethyl-allo-threonyl Hydroxamate-Based LpxC Inhibitor LPC-058. *The Journal of Organic Chemistry* **2016,** *81* (10), 4393-4398.

30.   Voynikov, Y.; Peikov, P.; Tencheva, J.; Zlatkov, A.; Stavrakov, G., *Synthesis and pharmacological properties of glutamic acid amides: A review*. 2012; Vol. 59, p 85-95.
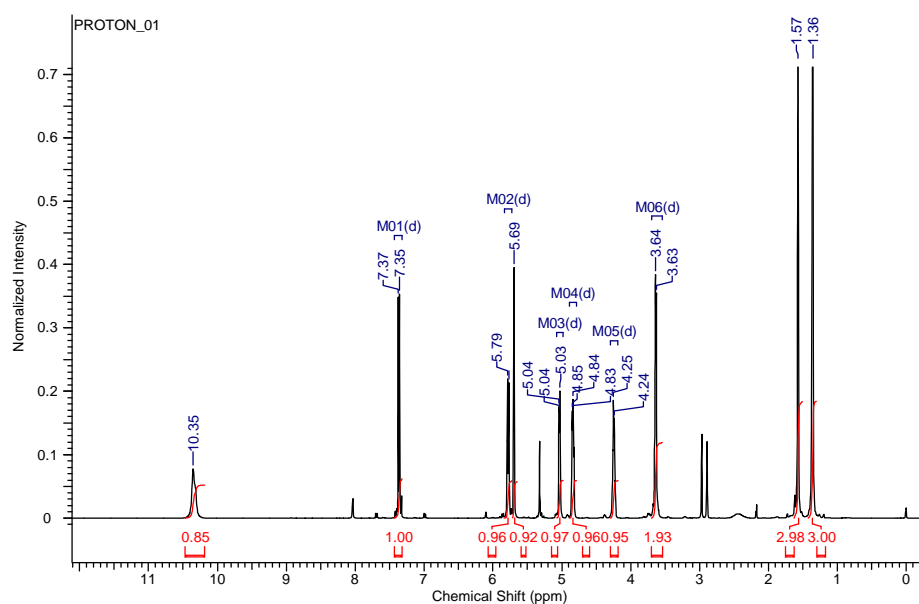
Appendix
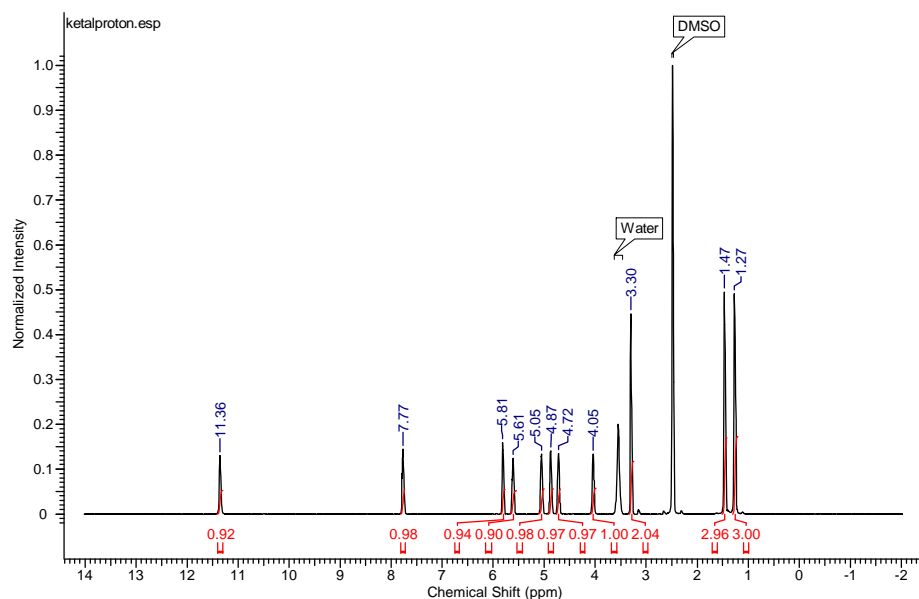
Figure A1. ^{1}HNMR of 1-((3aR,4R,6R,6aR)-6-(hydroxymethyl)-2,2-dimethyltetrahydrofuro[3,4-d][1,3]dioxol-4-yl)pyrimidine-2,4(1H,3H)-dione (**1**). ^{1}HNMR (400 MHz, DMSO): δ 1.27 (s, 3 H), 1.47 (s, 3 H), 3.30 (s, 2 H), 4.05 (s, 1 H), 4.72 (s, 1 H), 4.87 (s, 1 H), 5.05 (s, 1 H), 5.61 (s, 1 H), 5.81 (s, 1 H), 7.77 (s, 1 H), 11.36 (s, 1 H)
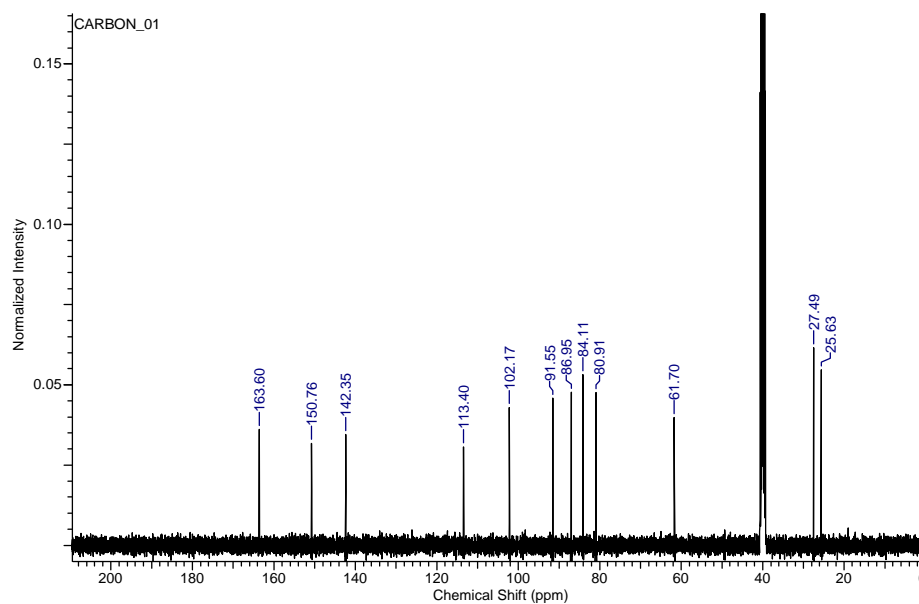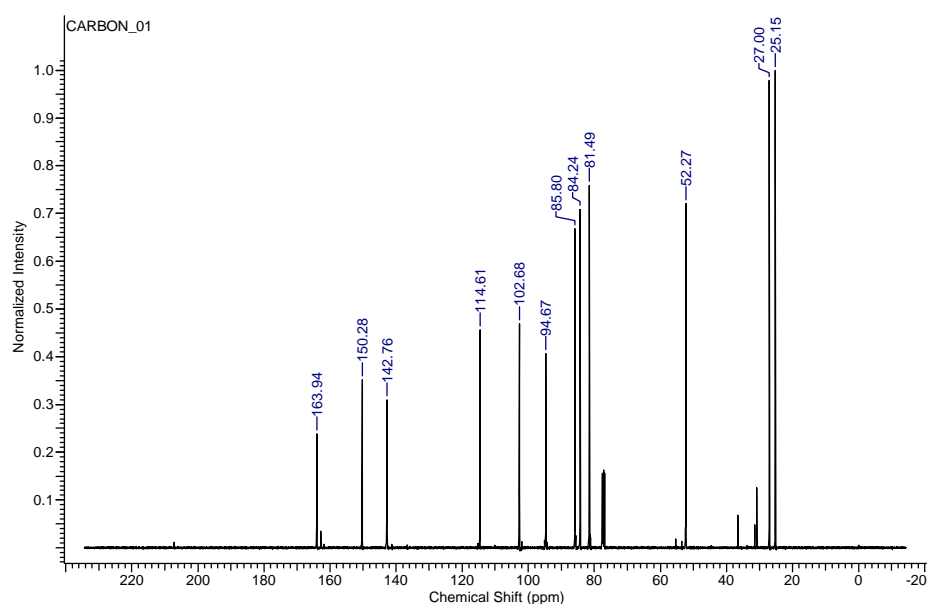

Figure A2. ^{13}CNMR of 1-((3aR,4R,6R,6aR)-6-(hydroxymethyl)-2,2-dimethyltetrahydrofuro[3,4-d][1,3]dioxol-4-yl)pyrimidine-2,4(1H,3H)-dione (**1**). ^{13}CNMR (100.5 MHz, DMSO): δ 25.63, 27.49, 61.70, 80.91, 84.11, 86.95, 91.55, 102.17, 113.40, 142.35, 150.76, 163.60
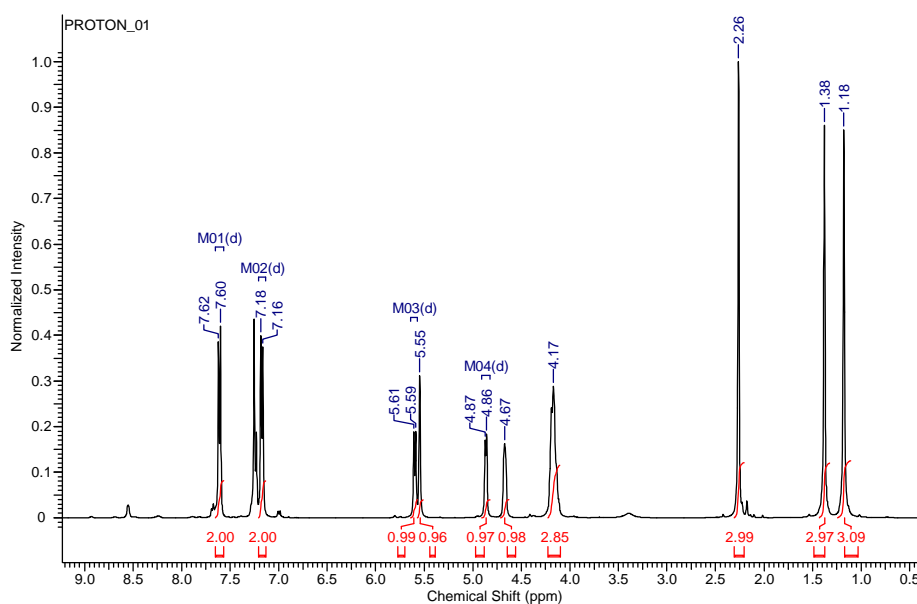
Figure A3. ¹HNMR of ((3aR,4R,6R,6aR)-6-(2,4-dioxo-3,4-dihydropyrimidin-1(2H)-yl)-2,2-dimethyltetrahydrofuro[3,4-d][1,3]dioxol-4-yl)methyl 4-methylbenzenesulfonate (**2**).
¹HNMR (400 MHz, CDCl3): δ 1.18 (s, 3 H), 1.38 (s, 3 H), 2.26 (s, 3 H), 4.17 (s, 3 H),
4.67 (s, 1 H), 4.87 (d, J = 6.3, 1 H), 5.60 (d, J = 7.8, 1 H), 7.17 (d, J = 8.2, 2 H), 7.61 (d, J = 8.2, 2 H)
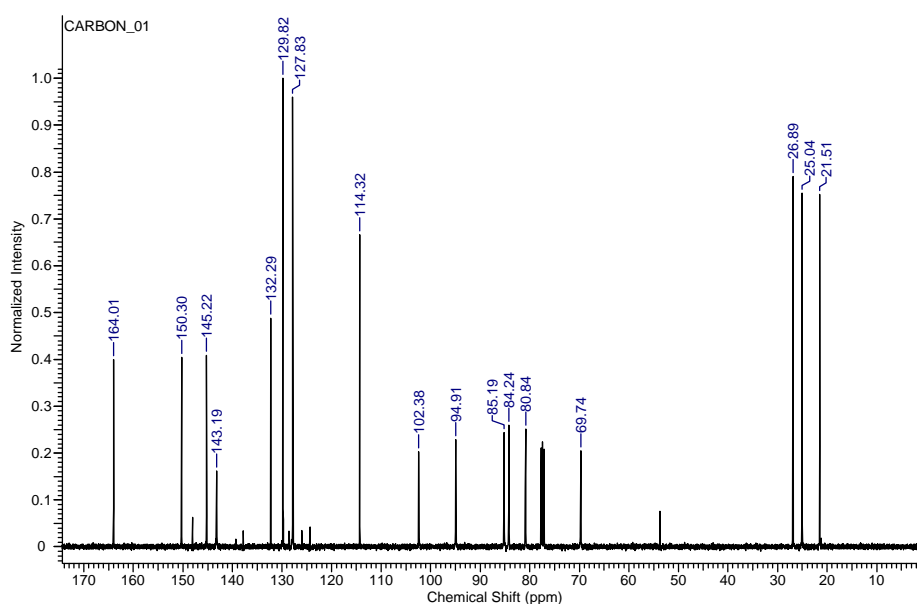
Figure A4. ¹³CNMR of ((3aR,4R,6R,6aR)-6-(2,4-dioxo-3,4-dihydropyrimidin-1(2H)-yl)-2,2-dimethyltetrahydrofuro[3,4-d][1,3]dioxol-4-yl)methyl 4-methylbenzenesulfonate (**2**).
¹³CNMR (100.5 MHz, CDCl3): δ 21.51, 25.04, 26.89, 69.74, 80.84, 84.24, 85.19, 94.91,
102.38, 114.32, 127.83, 129.82, 132.29, 143.19, 145.22, 150.30, 164.01

Figure A5. ^{1}HNMR of 1-((3aR,4R,6R,6aR)-6-(azidomethyl)-2,2-dimethyltetrahydrofuro[3,4-d][1,3]dioxol-4-yl)pyrimidine-2,4(1H,3H)-dione (**3**). ^{1}HNMR (400 MHz, CDCl$_3$): δ 1.36 (s, 3 H), 1.57 (s, 3 H), 3.63 (d, J = 4.7, 2 H), 4.24 (d, J = 4.3, 1 H), 4.84 (d, J = 5, 1 H), 5.04 (d, J = 7.2, 1 H), 5.78 (d, J = 7.8, 1 H), 5.79 (s, 1 H), 7.36 (d, J = 7.8, 1 H), 10.35 (s, 1 H)

Figure A6. ^{13}CNMR of 1-((3aR,4R,6R,6aR)-6-(azidomethyl)-2,2-dimethyltetrahydrofuro[3,4-d][1,3]dioxol-4-yl)pyrimidine-2,4(1H,3H)-dione (**3**). ^{13}CNMR (100.5 MHz, CDCl3): δ 25.15, 27.00, 52.27, 81.49, 84.24, 85.80, 94.67, 102.68, 114.61, 142.76, 150.28, 163.94
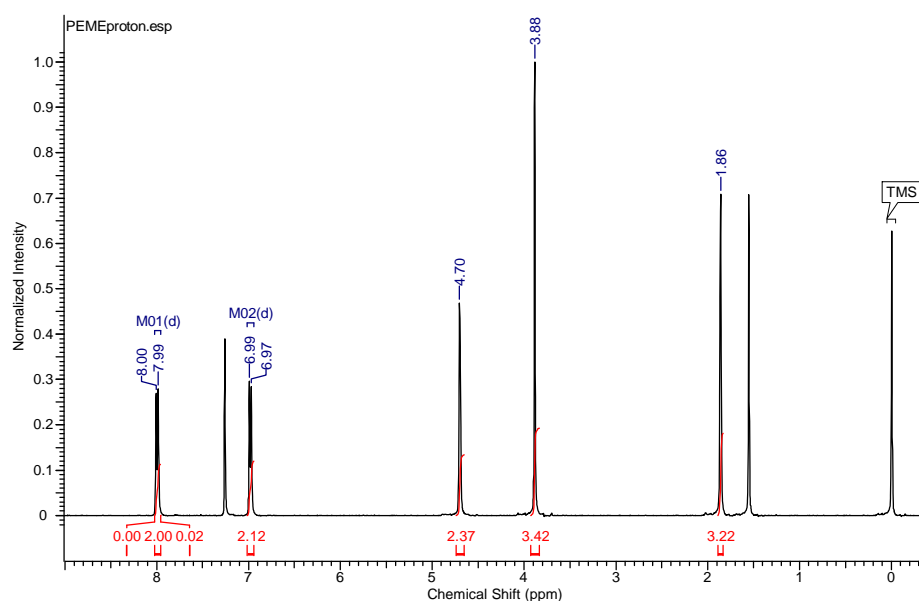
Figure A7. ^{1}HNMR of methyl 4-(but-2-yn-1-yloxy)benzoate (**4**). ^{1}HNMR (400 MHz, CDCl$_3$): δ 1.86 (s, 3 H), 3.88 (s, 3 H), 4.70 (s, 2 H), 6.98 (d, J = 7.8, 2 H), 7.99 (d, J = 7.8, 2 H)
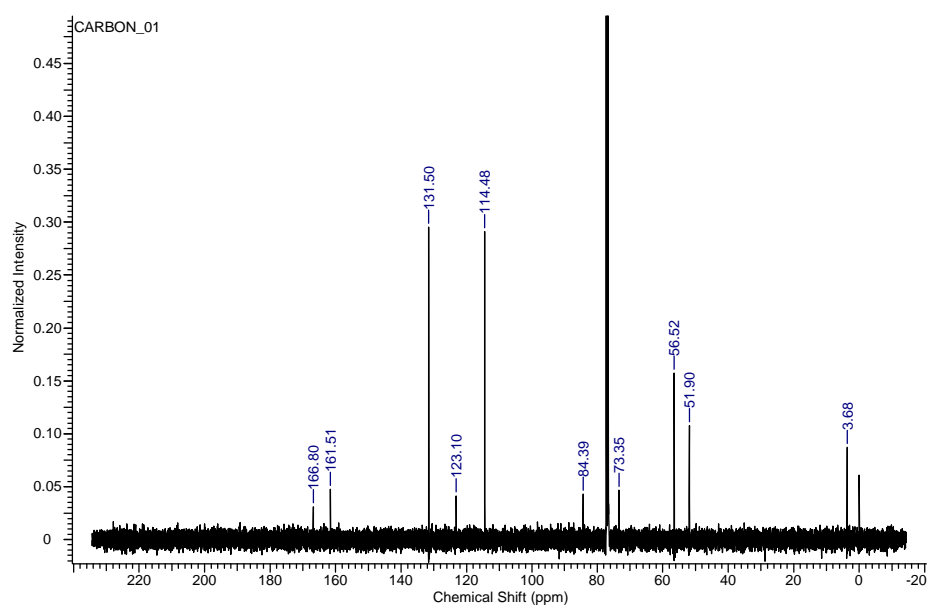
Figure A8. ^{13}CNMR of methyl 4-(but-2-yn-1-yloxy)benzoate (**4**). ^{13}CNMR (100.5 MHz, CDCl3): δ 3.68, 51.90, 56.52, 73.35, 84.39, 114.48, 123.10, 131.50, 161.51, 166.80
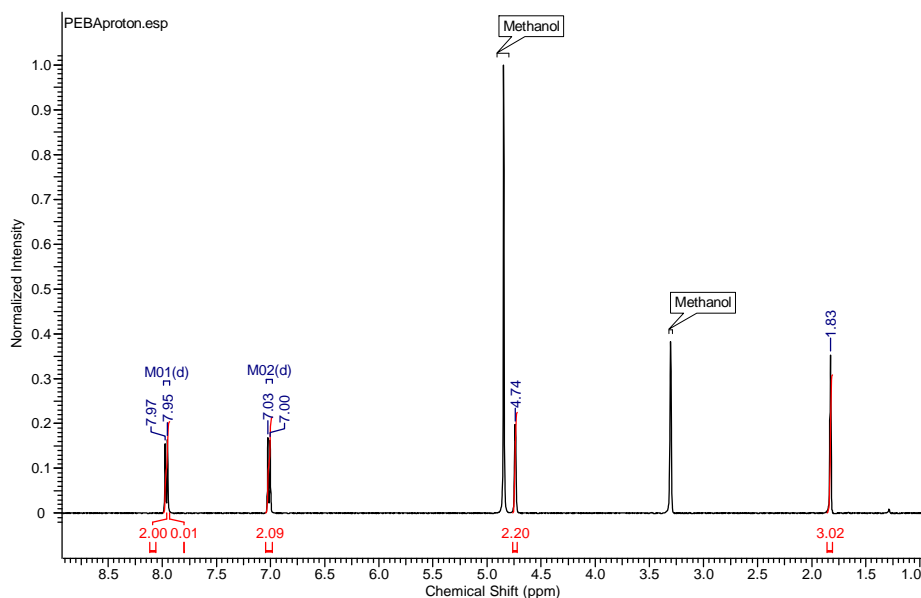
Figure A9. ^{1}HNMR of 4-(But-2-yn-1-yloxy)benzoic acid (**5**). ^{1}HNMR (400 MHz, CD$_3$OD): δ 1.83 (s, 3 H), 4.74 (s, 2 H), 7.03 (d, J = 9, 2 H), 7.95 (d, J = 9, 2 H)
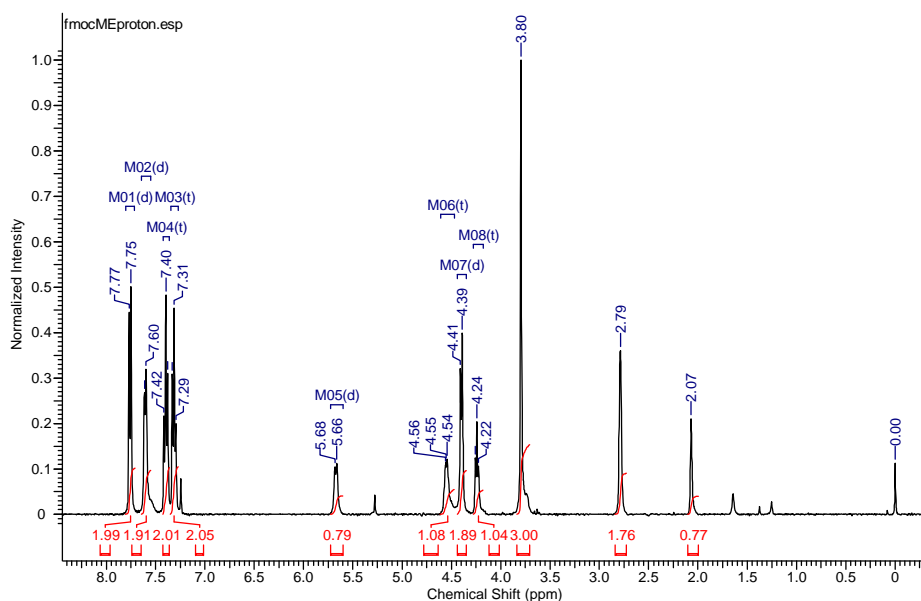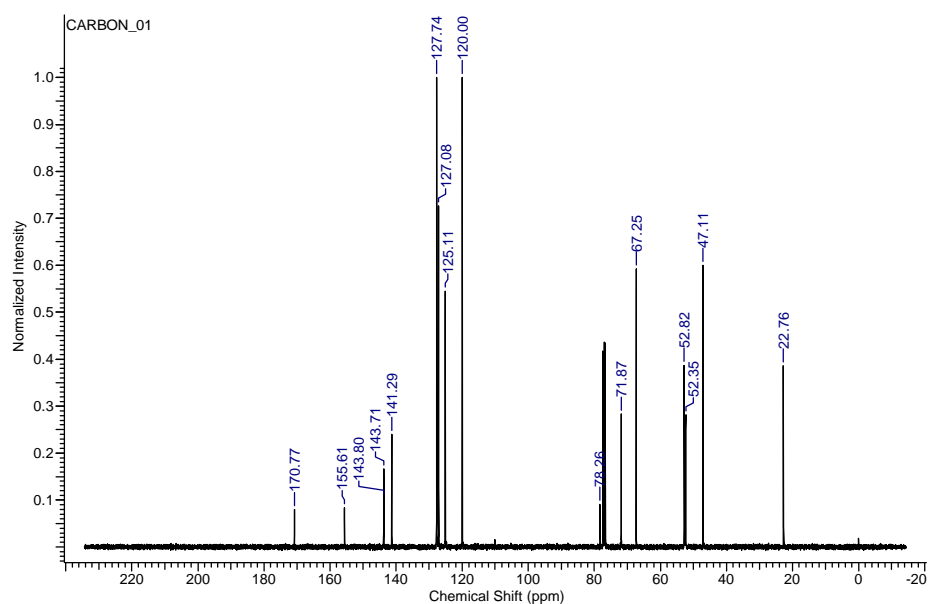

Figure A10. ^{1}HNMR of methyl (S)-2-((((9H-fluoren-9-yl)methoxy)carbonyl)amino)pent-4-ynoate (**8**). ^{1}HNMR (400 MHz, CDCl3): δ 2.07 (s, 1 H), 2.79 (s, 2 H), 3.80 (s, 3 H), 4.24 (t, J = 7(x2), 1 H), 4.40 (d, J = 7, 2 H), 4.55 (t, J = 4(x2), 1 H), 5.67 (d, J = 7.4, 1 H), 7.31 (t, J = 7(x2), 2 H), 7.40 (t, J = 7.4(x2), 2 H), 7.61 (d, J = 7, 2 H), 7.76 (d, J = 7.4, 2 H)

Figure A11. ^{13}CNMR of methyl (S)-2-((((9H-fluoren-9-yl)methoxy)carbonyl)amino)pent-4-ynoate (**8**). ^{13}CNMR (100.5 MHz, CDCl$_3$): δ 22.76, 47.11, 52.35, 52.82, 67.25, 71.87, 78.26, 120.00, 125.11, 127.08, 127.74, 141.29, 143.71, 143.80, 155.61, 170.77
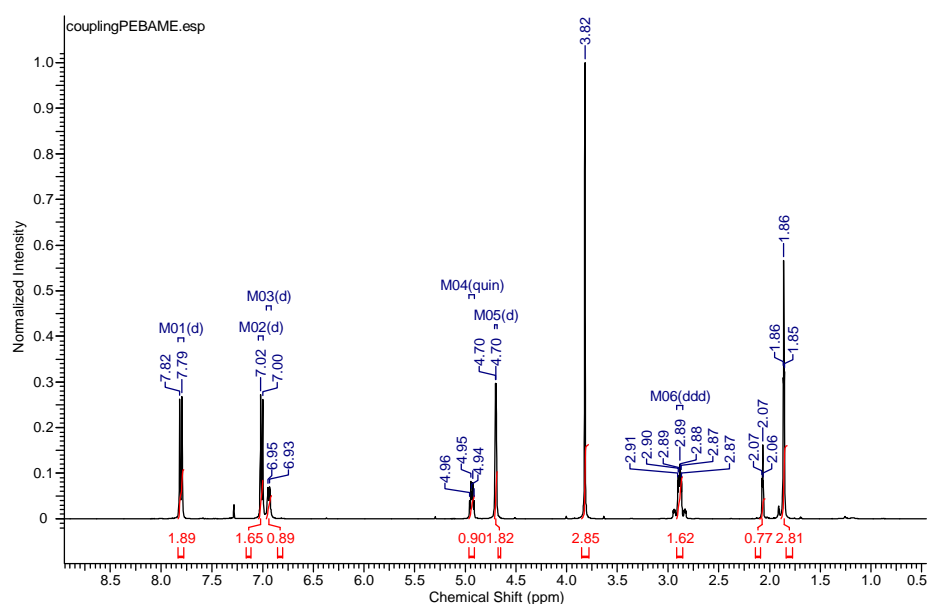

Figure A12. ^{1}HNMR of methyl (S)-2-(4-(but-2-yn-1-yloxy)benzamido)pent-4-ynoate (**9**). ^{1}HNMR (400 MHz, CDCl$_3$): δ 1.86 (s, 3 H), 2.07 (s, 1 H), 2.89 (ddd, J = 8.1, 4.8, 2.7, 2 H), 3.82 (s, 3 H), 4.70 (d, J = 2, 2 H), 4.94 (dt, J = 7.8, 4.7(x2), 1 H), 6.94 (d, J = 7.4, 1 H), 7.01 (d, J = 9, 2 H), 7.81 (d, J = 9, 2 H)
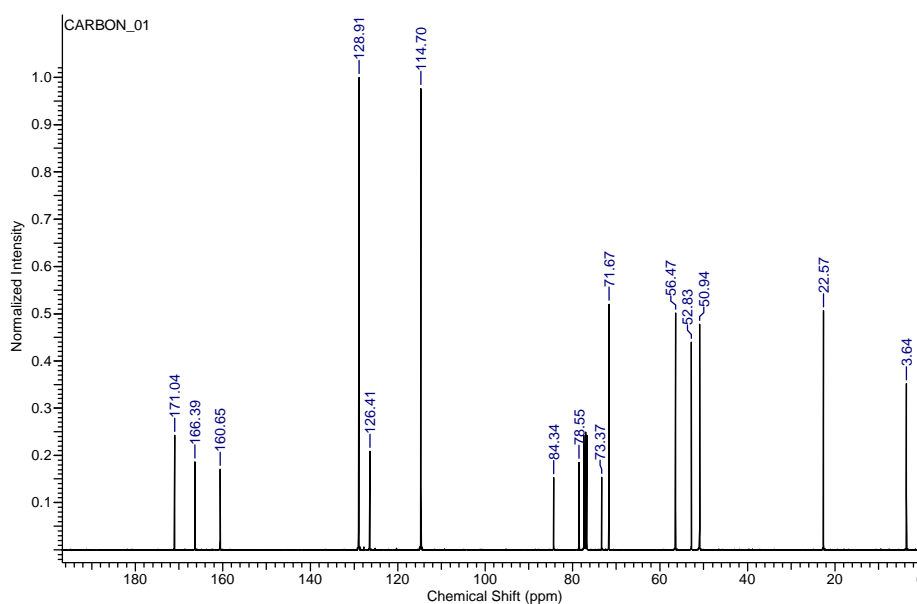
Figure A13. ^{13}CNMR of methyl (S)-2-(4-(but-2-yn-1-yloxy)benzamido)pent-4-ynoate (**9**). ^{13}CNMR (100.5 MHz, CDCl$_3$): δ 3.64, 22.57, 50.94, 52.83, 56.47, 71.67, 73.37, 78.55, 84.34, 114.70, 126.41, 128.91, 160.65, 166.39, 171.04
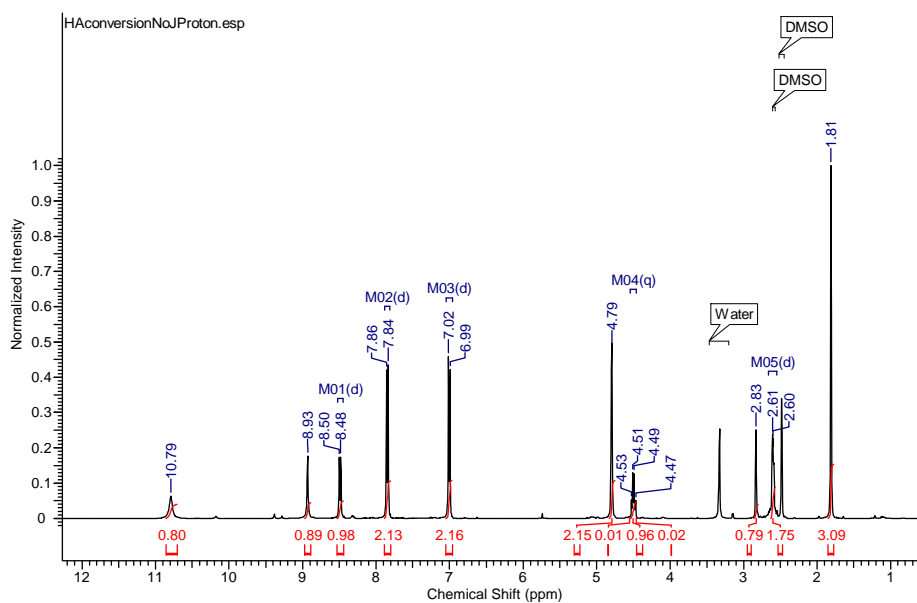

Figure A14. ^{1}HNMR of (S)-4-(But-2-yn-1-yloxy)-N-(1-(hydroxyamino)-1-oxopent-4-yn-2-yl)benzamide (**10**). ^{1}HNMR (400 MHz, DMSO): δ 1.81 (s, 3 H), 2.61 (d, *J* = 2.7, 2 H), 2.83 (s, 1 H), 4.50 (q, *J* = 7.6 (x3), 1 H), 4.79 (s, 2 H), 7.00 (d, *J* = 8.6, 2 H), 7.85 (d, *J* = 9, 2 H), 8.49 (d, *J* = 8.2, 1 H), 8.93 (s, 1 H), 10.79 (s, 1 H)
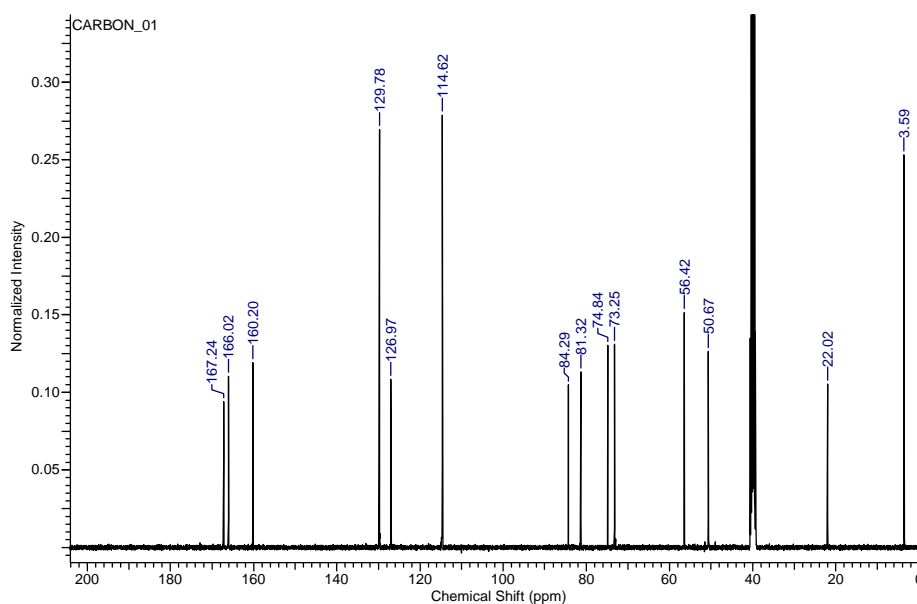
Figure A15. : ¹HNMR of (S)-4-(But-2-yn-1-yloxy)-N-(1-(hydroxyamino)-1-oxopent-4-yn-2-yl)benzamide (**10**).¹³CNMR (100.5 MHz, DMSO): δ 3.59, 22.02, 50.67, 56.42, 73.25, 74.84, 81.32, 84.29, 114.62, 126.97, 129.78, 160.20, 166.02, 167.24
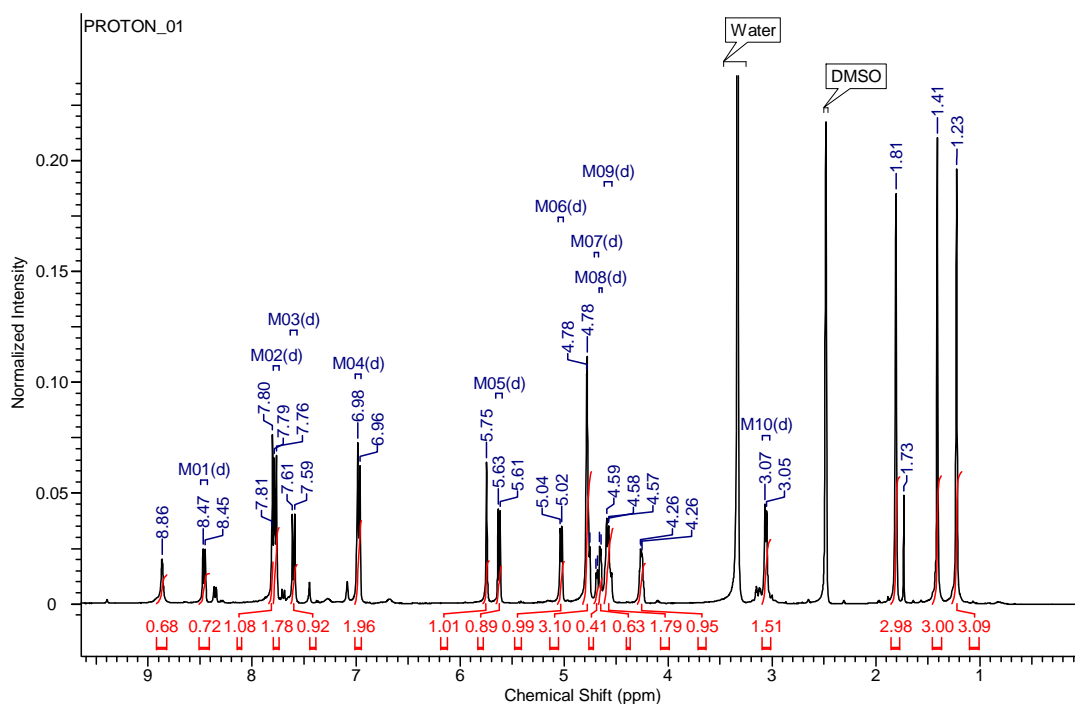

Figure A16. ¹HNMR of 4-(But-2-yn-1-yloxy)-N-((S)-3-(1-(((3aR,4R,6R,6aR)-6-(2,4-dioxo-3,4-dihydropyrimidin-1(2H)-yl)-2,2-dimethyltetrahydrofuro[3,4-d][1,3]dioxol-4-yl)methyl)-1H-1,2,3-triazol-4-yl)-1-(hydroxyamino)-1-oxopropan-2-yl)benzamide (**11**). ¹HNMR (400 MHz, DMSO): δ 1.23 (s, 3 H), 1.41 (s, 3 H), 1.81 (s, 3 H), 3.06 (d, *J* = 7, 2 H), 4.26 (m, 1 H), 4.58 (d, *J* = 8.3, 2 H), 4.65 (d, *J* = 4.3, 1 H), 4.69 (d, *J* = 4.7, 1 H), 4.78 (s, 3 H), 5.03 (d, *J* = 6.3, 1 H), 5.62 (d, *J* = 7.8, 1 H), 5.75 (s, 1 H), 6.97 (d, *J* = 8.6, 2 H),

7.60 (d, J = 8.2, 1 H), 7.78 (d, J = 8.6, 2 H), 7.80 (s, 1 H), 8.46 (d, J = 8.2, 1 H), 8.86 (s, 1 H)
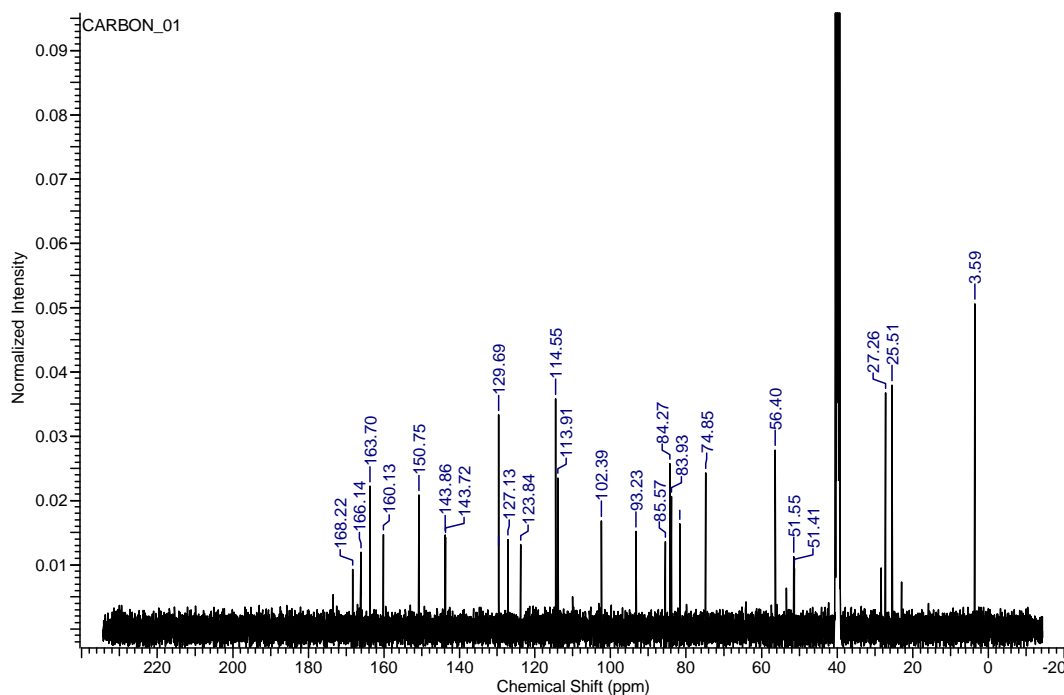

Figure A17. ^{13}CNMR of 4-(But-2-yn-1-yloxy)-N-((S)-3-(1-(((3aR,4R,6R,6aR)-6-(2,4-dioxo-3,4-dihydropyrimidin-1(2H)-yl)-2,2-dimethyltetrahydrofuro[3,4-d][1,3]dioxol-4-yl)methyl)-1H-1,2,3-triazol-4-yl)-1-(hydroxyamino)-1-oxopropan-2-yl)benzamide (**11**).
^{13}CNMR (100.5 MHz, DMSO): δ 3.59, 25.51, 27.26, 51.41, 56.39, 74.85, 81.58, 83.93, 84.26, 85.56, 93.23, 102.38, 113.91, 114.55, 123.84, 127.13, 129.68, 143.72, 143.85, 150.74, 160.12, 163.70, 166.15, 168.22
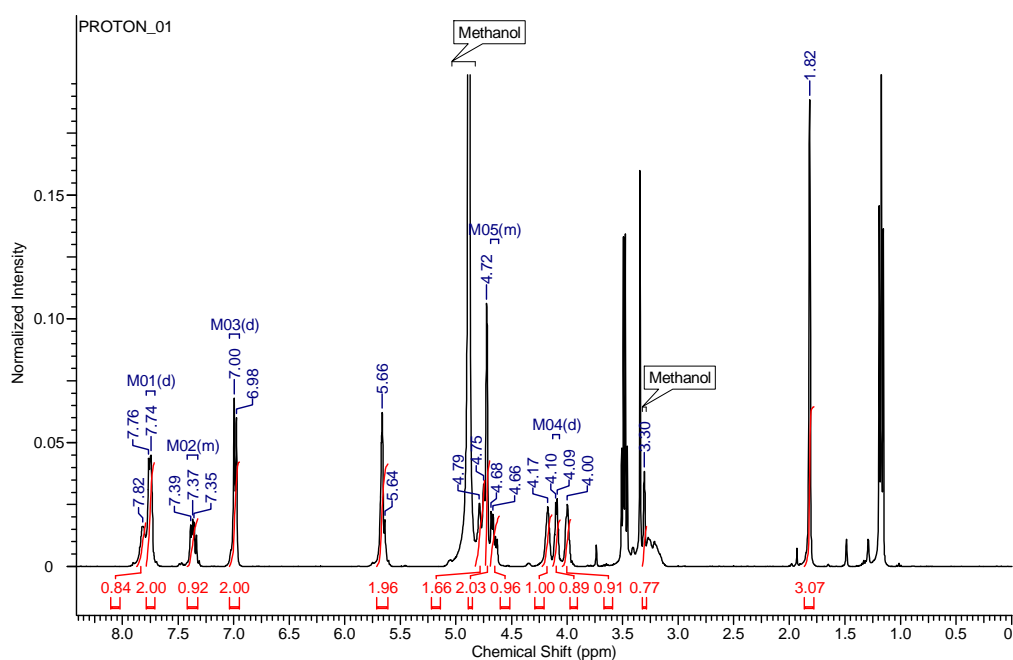
Figure A18. ^{1}HNMR of 4-(but-2-yn-1-yloxy)-N-((S)-3-(1-(((2R,3S,4R,5R)-5-(2,4-dioxo-3,4-dihydropyrimidin-1(2H)-yl)-3,4-dihydroxytetrahydrofuran-2-yl)methyl)-1H-1,2,3-triazol-4-yl)-1-(hydroxyamino)-1-oxopropan-2-yl)benzamide (**DP-001**). ^{1}HNMR (400 MHz, DMSO): δ 1.82 (s, 3 H), 3.30 (s, 1 H), 4.00 (s, 2 H), 4.09 (d, J = 4.7, 1 H), 4.17 (s, 1 H), 4.67 (m, 1 H), 4.72 (s, 2 H), 4.79 (s, 2 H), 5.66 (s, 2 H), 6.99 (d, J = 8.2, 2 H), 7.37 (m, 1 H), 7.75 (d, J = 7.8, 2 H), 7.82 (s, 1 H)
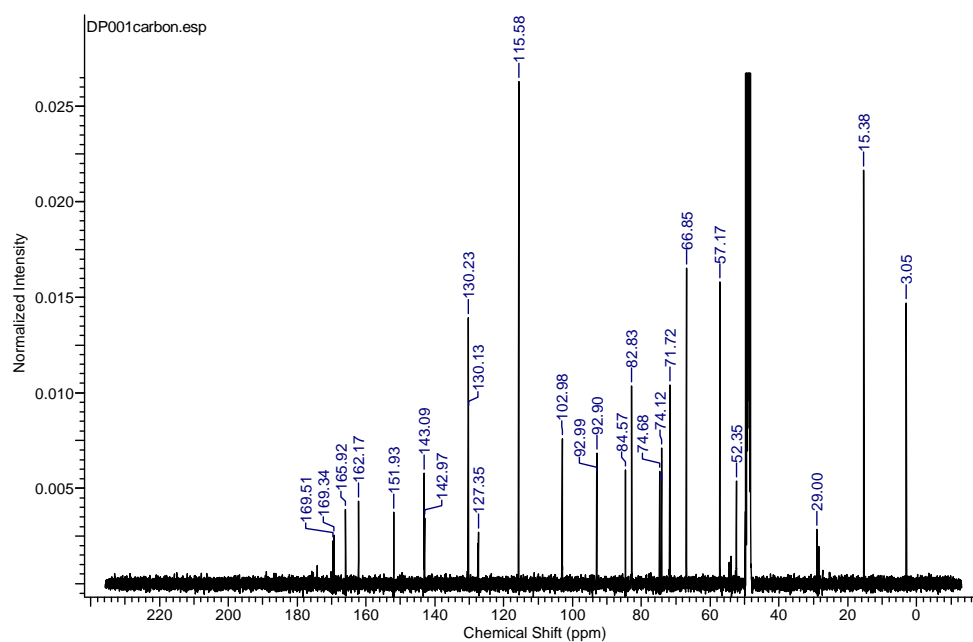
Figure A19. ^{13}CNMR of 4-(but-2-yn-1-yloxy)-N-((S)-3-(1-(((2R,3S,4R,5R)-5-(2,4-dioxo-3,4-dihydropyrimidin-1(2H)-yl)-3,4-dihydroxytetrahydrofuran-2-yl)methyl)-1H-1,2,3-triazol-4-yl)-1-(hydroxyamino)-1-oxopropan-2-yl)benzamide (**DP-001**). ^{13}CNMR (100.5 MHz, DMSO): δ 3.05, 29.00, 52.35, 57.17, 71.72, 74.12, 74.68, 82.83, 92.90, 102.98, 115.58, 127.35, 130.13, 130.23, 142.97, 143.09, 151.93, 162.17, 165.92, 169.34, 169.51